

UNCLASSIFIED

AD NUMBER
ADB263428
NEW LIMITATION CHANGE
TO Approved for public release, distribution unlimited
FROM Distribution authorized to U.S. Gov't. agencies only; Proprietary Info.; Oct 1999. Other requests shall be referred to US Army Medical Research and Materiel Comd., 504 Scott St., Fort Detrick, MD 21702-5012.
AUTHORITY
USAMRMC ltr, 23 Aug 2001

THIS PAGE IS UNCLASSIFIED

AD _____

Award Number: DAMD17-97-1-7344

TITLE: Pathogenesis of Germline and Somatic NF1 Rearrangements

PRINCIPAL INVESTIGATOR: Karen Stephens, Ph.D.

CONTRACTING ORGANIZATION: University of Washington
Seattle, Washington 98105-6613

REPORT DATE: October 1999

TYPE OF REPORT: Annual

PREPARED FOR: U.S. Army Medical Research and Materiel Command
Fort Detrick, Maryland 21702-5012

DISTRIBUTION STATEMENT: Distribution authorized to U.S.
Government agencies only (proprietary information, Oct 99).
Other requests for this document shall be referred to U.S.
Army Medical Research and Materiel Command, 504 Scott Street,
Fort Detrick, Maryland 21702-5012.

The views, opinions and/or findings contained in this report are those
of the author(s) and should not be construed as an official Department
of the Army position, policy or decision unless so designated by other
documentation.

NOTICE

USING GOVERNMENT DRAWINGS, SPECIFICATIONS, OR OTHER DATA INCLUDED IN THIS DOCUMENT FOR ANY PURPOSE OTHER THAN GOVERNMENT PROCUREMENT DOES NOT IN ANY WAY OBLIGATE THE U.S. GOVERNMENT. THE FACT THAT THE GOVERNMENT FORMULATED OR SUPPLIED THE DRAWINGS, SPECIFICATIONS, OR OTHER DATA DOES NOT LICENSE THE HOLDER OR ANY OTHER PERSON OR CORPORATION; OR CONVEY ANY RIGHTS OR PERMISSION TO MANUFACTURE, USE, OR SELL ANY PATENTED INVENTION THAT MAY RELATE TO THEM.

LIMITED RIGHTS LEGEND

Award Number: DAMD17-97-1-7344

Organization: University of Washington

Those portions of the technical data contained in this report marked as limited rights data shall not, without the written permission of the above contractor, be (a) released or disclosed outside the government, (b) used by the Government for manufacture or, in the case of computer software documentation, for preparing the same or similar computer software, or (c) used by a party other than the Government, except that the Government may release or disclose technical data to persons outside the Government, or permit the use of technical data by such persons, if (i) such release, disclosure, or use is necessary for emergency repair or overhaul or (ii) is a release or disclosure of technical data (other than detailed manufacturing or process data) to, or use of such data by, a foreign government that is in the interest of the Government and is required for evaluational or informational purposes, provided in either case that such release, disclosure or use is made subject to a prohibition that the person to whom the data is released or disclosed may not further use, release or disclose such data, and the contractor or subcontractor or subcontractor asserting the restriction is notified of such release, disclosure or use. This legend, together with the indications of the portions of this data which are subject to such limitations, shall be included on any reproduction hereof which includes any part of the portions subject to such limitations.

THIS TECHNICAL REPORT HAS BEEN REVIEWED AND IS APPROVED FOR PUBLICATION.

N. Minichew
01/19/2001

REPORT DOCUMENTATION PAGEForm Approved
OMB No. 074-0188

Public reporting burden for this collection of information is estimated to average 1 hour per response, including the time for reviewing instructions, searching existing data sources, gathering and maintaining the data needed, and completing and reviewing this collection of information. Send comments regarding this burden estimate or any other aspect of this collection of information, including suggestions for reducing this burden to Washington Headquarters Services, Directorate for Information Operations and Reports, 1215 Jefferson Davis Highway, Suite 1204, Arlington, VA 22202-4302, and to the Office of Management and Budget, Paperwork Reduction Project (0704-0188), Washington, DC 20503

1. AGENCY USE ONLY (Leave blank)		2. REPORT DATE October 1999	3. REPORT TYPE AND DATES COVERED Annual (30 Sep 98 - 29 Sep 99)	
4. TITLE AND SUBTITLE Pathogenesis of Germline and Somatic NF1 Rearrangements			5. FUNDING NUMBERS DAMD17-97-1-7344	
6. AUTHOR(S) Karen Stephens, Ph.D.				
7. PERFORMING ORGANIZATION NAME(S) AND ADDRESS(ES) University of Washington, Seattle, Washington 98105-6613 e-mail: millie@u.washington.edu			8. PERFORMING ORGANIZATION REPORT NUMBER	
9. SPONSORING / MONITORING AGENCY NAME(S) AND ADDRESS(ES) U.S. Army Medical Research and Materiel Command Fort Detrick, Maryland 21702-5012			10. SPONSORING / MONITORING AGENCY REPORT NUMBER	
11. SUPPLEMENTARY NOTES				
12a. DISTRIBUTION / AVAILABILITY STATEMENT DISTRIBUTION STATEMENT: Distribution authorized to U.S. Government agencies only (proprietary information, Oct 99). Other requests for this document shall be referred to U.S. Army Medical Research and Materiel Command, 504 Scott Street, Fort Detrick, Maryland 21702-5012.				12b. DISTRIBUTION CODE
13. ABSTRACT (Maximum 200 Words) We have determined that very unusual chromosomal rearrangements involving the NF1 gene occur in both germline and somatic tissues of certain patients. Germline microdeletions of 1.5 Mb are caused by recombination between repeated elements that flank the NF1 gene. Our data support the hypothesis of a co-deletion of NF1 and a novel gene that potentiates neurofibromagenesis and narrow the location of this gene. We describe detailed clinical description of 20 NF1 deletion patientse, which suggest that NF1 microdeletion may be predictive of phenotype. We have developed an automated PCR-based dosage assay to rapidly identify and map the extent of NF1 deletions, which should be directly applicable to diagnostic testing of patients. We describe for the first time somatic rearrangements in tumor cells that arise by double mitotic recombination with clustered breakpoints. These rearrangements result in interstitial isodisomy for a 50 Mb region chromosome 17 and occurred in leukemic tumors of children with NF1 and myeloid dysplasia. Because both the germline and somatic rearrangements involve not only the NF1 gene but many other genes, our data implicate other elements/loci that play an important role in sporadic cases of NF1 and in somatic loss of NF1 during leukemogenesis and possibly during other NF1-associated neoplasias.				
14. SUBJECT TERMS Neurofibromatosis			15. NUMBER OF PAGES 74	
			16. PRICE CODE	
17. SECURITY CLASSIFICATION OF REPORT Unclassified	18. SECURITY CLASSIFICATION OF THIS PAGE Unclassified	19. SECURITY CLASSIFICATION OF ABSTRACT Unclassified	20. LIMITATION OF ABSTRACT Unlimited	

FOREWORD

Opinions, interpretations, conclusions and recommendations are those of the author and are not necessarily endorsed by the U.S. Army.

_____ Where copyrighted material is quoted, permission has been obtained to use such material.

_____ Where material from documents designated for limited distribution is quoted, permission has been obtained to use the material.

_____ Citations of commercial organizations and trade names in this report do not constitute an official Department of Army endorsement or approval of the products or services of these organizations.

_____ In conducting research using animals, the investigator(s) adhered to the "Guide for the Care and Use of Laboratory Animals," prepared by the Committee on Care and use of Laboratory Animals of the Institute of Laboratory Resources, national Research Council (NIH Publication No. 86-23, Revised 1985).

N/A For the protection of human subjects, the investigator(s) adhered to policies of applicable Federal Law 45 CFR 46.

N/A In conducting research utilizing recombinant DNA technology, the investigator(s) adhered to current guidelines promulgated by the National Institutes of Health.

N/A In the conduct of research utilizing recombinant DNA, the investigator(s) adhered to the NIH Guidelines for Research Involving Recombinant DNA Molecules.

X In the conduct of research involving hazardous organisms, the investigator(s) adhered to the CDC-NIH Guide for Biosafety in Microbiological and Biomedical Laboratories.

Karen B. Stephens 10/26/99
PI - Signature Date

4. Table of Contents

<u>Item #</u>	<u>Description</u>	<u>Page</u>
1	Front Cover	
2	Standard Form 298	2
3	Foreword	3
4	Table of Contents	4
5	Introduction	5
6	Body	5
7	Key Research Accomplishments	25
8	Reportable Outcomes	25
9	Conclusions	26
10	References	27
11	Appendices	27

5. Introduction

Neurofibromatosis type 1 is a common autosomal dominant tumor-susceptibility disorder (Mulvihill, 1994). Virtually every affected individual develops benign cutaneous neurofibromas, while the development of other tumors such as plexiform neurofibromas, malignant myeloid disorders, and neurofibrosarcomas are a less common complication (Riccardi, 1993; Shannon *et al.*, 1994). The subject of this research project is to investigate the genetic mechanisms and pathology underlying both germline and somatic microdeletions involving the NF1 gene. Two hypotheses will be tested. In 1994, we hypothesize that the early age at onset of cutaneous neurofibromas observed in patients with a germline NF1 microdeletion (Kayes *et al.*, 1994; Kayes *et al.*, 1992; Leppig *et al.*, 1997; Leppig *et al.*, 1996; Wu *et al.*, 1997; Wu *et al.*, 1995) was due to co-deletion of another gene that potentiates neurofibromagenesis. To test this hypothesis, we will ascertain additional deletion patients, construct a fine map of the region, map each patient's deletion breakpoints, and look for genotype/phenotype correlations. Secondly, children with NF1 are at increased risk of malignant myeloid disorders (Miles *et al.*, 1997; Mulvihill, 1994; Shannon *et al.*, 1994). Among such cases, approximately 50% of the primary leukemic cells showed loss of constitutional heterozygosity (LOH) at the NF1 locus (Shannon *et al.*, 1994). We recently identified a patient whose LOH resulted from the novel somatic rearrangement of interstitial isodisomy, presumably due to double mitotic recombination. The novelty of this rearrangement led us to hypothesize that it may be a frequent mechanism of LOH at the NF1 locus and/or contribute directly to leukemogenesis. To test this hypothesis, we proposed to ascertain additional patients, map the loci on chromosome 17 that showed LOH, determine parental origin of allelic loss, and determine the underlying molecular mechanism of the somatic rearrangements and their contribution to malignancy.

6. Body

A. Progress on Technical Objective 1: To identify additional patients with large germline NF1 deletions.

- Task 1: Months 1-6: develop and optimize an NF1 gene dosage PCR assay for detecting deletions at the 5' end of the gene.
- Task 2: Months 4-7: assay the ~105 DNA samples currently in the lab for 3' NF1 deletions.
- Task 3: Months 1-25: obtain pathological tissue samples or purified DNA from NF1 clinic patients; perform the 5' and 3' NF1 gene dosage PCR assays for all samples; calculate the NF1 gene dosage to identify deletion patients.
- Task 4: Months 20-25: Determine the frequency of NF1 deletions. Write a manuscript on deletion screening protocol and frequency.

The timeline for accomplishing Objective 1 was altered for 3 important reasons. First, we chose to focus on and complete Objective 2 and 3 (see below) because samples were available earlier than expected and the results were so exciting. Second, the results from objective 2 will facilitate designing optimal gene dosage assays for screening. Third, we chose to wait for delivery of a new instrument that we can use to development of an automated gene dosage PCR assay.

a. [Tasks 2 & 3]. We have begun screening our collection of NF1 patients and have identified additional patients with NF1 microdeletions. This screening was performed using the manual NF1 PCR gene dosage assay developed in my laboratory (Figures 1 and 2).

A manuscript detailing these results was submitted. The reviewers requested additional clinical information on the new deletion patients. After considerable efforts to obtain, this information is now being incorporated into the revised manuscript. K. Maruyama, M. Weaver, K.A. Leppig, R. Farber, A. Aylsworth, Michael Dorschner, J. Ortenberg, A. Rubenstein, L. Immken, E. Haan, C. Curry and K. Stephens. Quantitative PCR gene dosage assay for detection of NF1 contiguous gene deletions. Submitted, in revision.

b. [Tasks 1 & 3]. The detailed physical map of the deleted region (see Objective 2 below) permits us to design gene dosage assays to specifically detect patients with breakpoints in the NF1REP regions or patients with novel breakpoints. Specific assays will facilitate the identification of patients with novel deletions thereby allowing us to deletion map the location of the putative gene that potentiates neurofibromagenesis. Our previous gene dosage assay for exon 32 of the NF1 gene was performed manually with radioactive labeling, co-amplification of cloned control sequences, gel electrophoresis, and quantitation of product by phosphorimage analysis. To bypass the significant time required to construct and clone the proper control sequences for each locus, and the time consuming aspects of the assay, we have developed an automated fluorescent PCR gene dosage assay that can quickly be adapted for NF1 or even anonymous loci across the deleted region.

BEGIN PROPRIETARY INFORMATION.

Automated gene dosage assay. The accumulation of PCR product during amplification can be quantitated by measuring the increase in fluorescence of a dye such as SYBR green I when bound to double-stranded DNA. Real-time detection of PCR is accomplished with the use of an ABI sequence detection system 7700, which has a built-in thermal cycler. Fluorescence emissions are guided through 96 individual fiber optic cables after excitation by a laser and detected by a CCD camera. The amount of SYBR green fluorescence is compared to an internal passive reference, ROX, during each PCR cycle. During the initial cycles of amplification, little or no change in fluorescence is detected, which represents a baseline. When the fluorescence signal reaches a fixed threshold above the baseline, a fractional CT (threshold cycle) can be determined. The comparison of CT values between a control disomic locus and a target locus can be used to determine the relative quantity or starting copy number of a given template. Alternatively, a standard curve can be constructed using CT values allowing for more absolute quantitation. Adaptation of this technology to determine gene copy number is a rapid and inexpensive alternative to conventional, isotopic methods.

We have developed a SYBR green gene dosage assay to detect NF1 microdeletions from genomic DNA. Primers designed to amplify a 55 bp fragment of exon 32 of the NF1 gene and another set specific to a 53 bp segment of exon 8 of the LIS1 (Lisencephaly 1) locus are used to determine the copy number of the NF1 gene. LIS1 is used as the disomic control because all living individuals would be disomic at this locus. To determine whether a patient is disomic or monosomic for NF1, a comparative CT calculation is made. First, the difference of CT values for LIS1 and NF1 is determined for a sample known to be disomic for NF1. Second, the same calculation is made for an "unknown" sample. These "difference"

values are used in the standard formula, $2^{-\Delta\Delta CT}$ (Figure 3). Values near 0.5 would represent NF1 monosomy, while values approaching 1.0 would designate disomy. We have established reference ranges for monosomy ranging from 0.35 to 0.65 and disomy from 0.85 to 1.15. A sample of the ABI SDS 7700 data output and comparative CT calculation for the NF1 exon 32 assay is shown in Figure 3. In addition, we have developed two similar assays for the EST loci SGC34232 and IB518, which are located ~200 kb on either side of the NF1 gene (Figure 4 below). The dosage values of these loci can be used to determine whether an entire copy of the NF1 gene has been deleted or possibly a portion of the gene.

Adaptation of this technology to determine gene copy number provides a rapid and inexpensive alternative to conventional, isotopic methods. Since this system directly examines copy number of a given locus, reliance on the informativeness of polymorphic loci commonly used for loss of heterozygosity studies is eliminated. New dosage markers can also be developed very quickly.

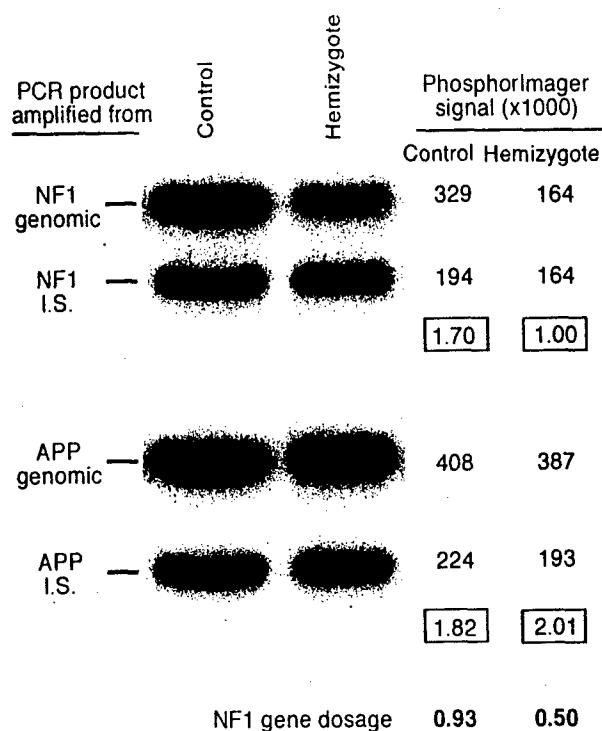
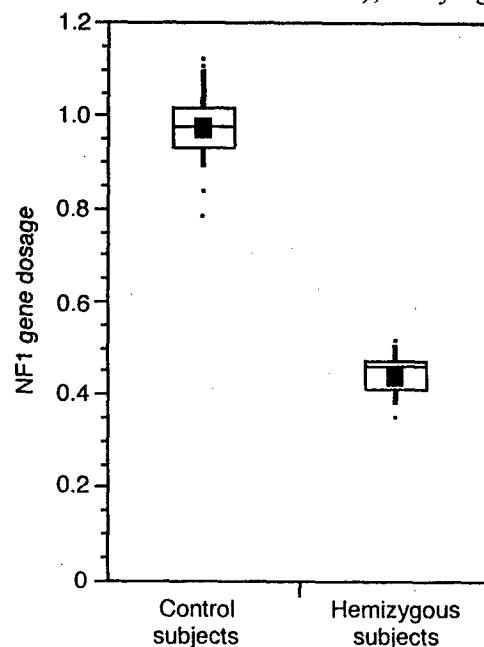
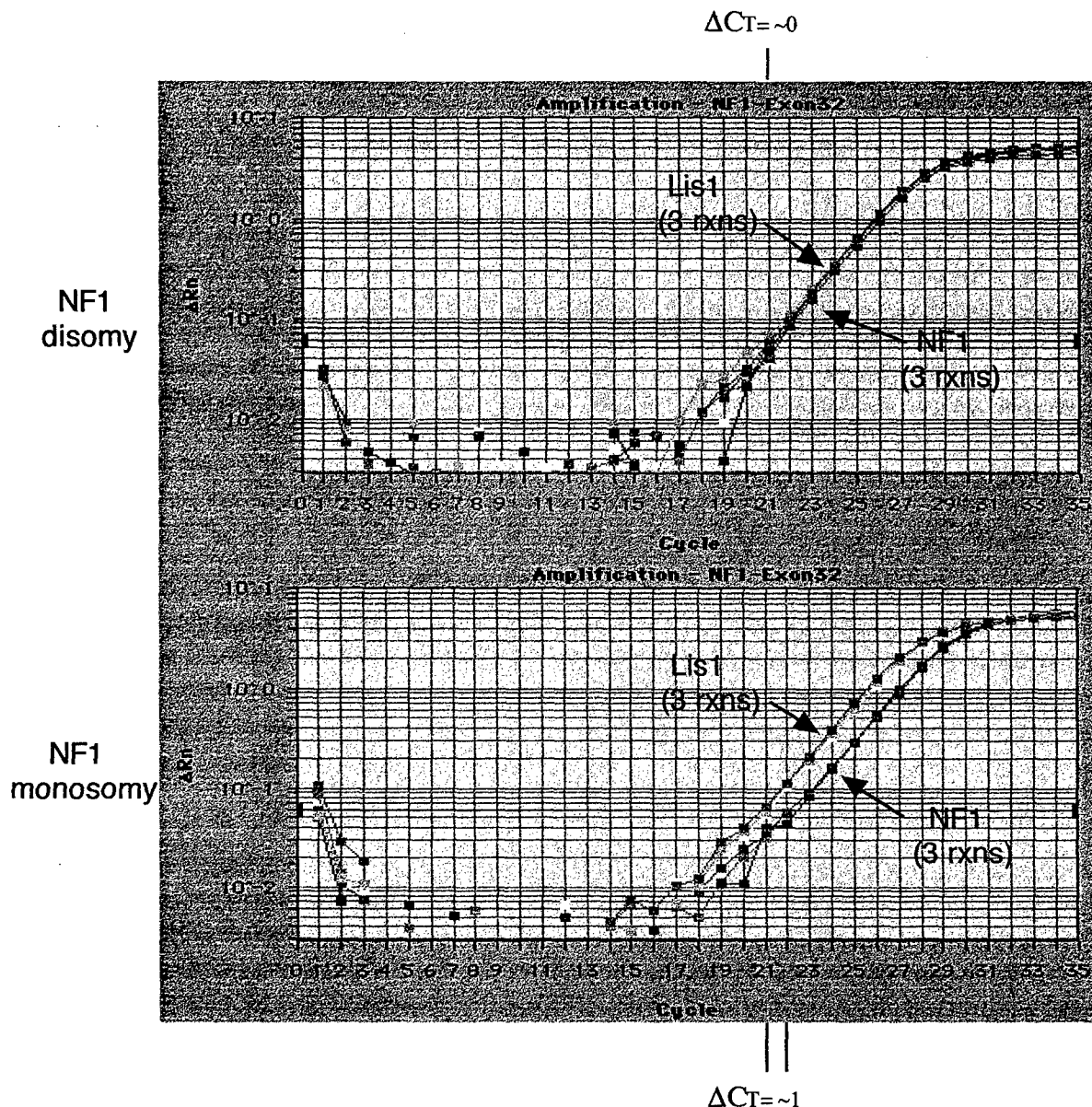


Figure 1. Example of the *NF1* gene dosage PCR assay. The four products of the assay are 310 bp *NF1* and 232 bp *APP* fragments amplified from the subject's genomic DNA and 290 and 212 bp fragments amplified from the internal standard (I.S.) sequences in plasmids pKM204 and pKM201, which were spiked into the reaction. An autoradiograph is shown for illustration purposes only, products were quantitated by phosphorimage analysis. The ratio of genomic to I.S. product for each gene (boxed values) and the *NF1* gene dosage (bold value), which is the quotient of the ratio of *NF1* products over the ratio of *APP* products (Celi et al. 1994), were calculated.

Figure 2. Distinct distributions of gene dosage values of *NF1* disomic and monosomic control subjects. Genomic DNA from 21 unaffected individuals (presumed disomic at *NF1*) and from 11 individuals monosomic for *NF1* were assayed as described in Materials and Methods. Although duplicate reactions were carried out for all samples, Figure 3 shows one randomly selected outcome per subject. Box plot indicators are: arithmetic mean (closed square), median (50%; horizontal line bisecting open box), upper and lower quartile (75% and 25%; top and bottom boundaries of open box, respectively), upper and lower decile (90% and 10%; upper and lower limits of vertical line); outlying data points (dots extending from vertical line).





A. Disomic control sample: B. Unknown sample: C. Calculate the dosage value:

Lis1 C_T - Ex32 $C_T = 0$

Lis1 C_T - Ex32 $C_T = 1$

21 - 21 = 0

21 - 22 = 1

$$2^{-\Delta\Delta C_T} = 2^{-(1-0)} = 0.5$$

therefore: $\Delta C_T = 0$

therefore: $\Delta C_T = 1$

A dosage value of .40 - .60 is consistent with NF1 monosomy

A dosage value of .85 - 1.10 is consistent with NF1 disomy

Figure 3 : Data output and sample comparative C_T calculation. The panels above show data output from the ABI SDS 7700. Each PCR reaction is run in triplicate and an average C_T is used for dosage calculations. The almost complete overlap of the amplification curves demonstrates the reproducibility of the reactions. Comparison of the amplification curves between NF1 disomy and monosomy shows a shift of the NF1 curve from left to right indicating the additional cycle(s) required to reach the C_T threshold due to the difference in NF1 copy number.

END OF PROPRIETARY INFORMATION.

B. Progress on Technical Objective 2: Identify a critical deletion region associated with early onset of neurofibromas.

- Task 1: Months 1-12: Map the location of additional loci to the *NF1* region by somatic cell hybrid analysis; identify any physical intervals that lack markers.
- Task 2: Month 13-14: Write a manuscript describing the physical map of the *NF1* region; assess the need for identification and mapping of new marker loci to certain physical intervals. If necessary, obtain YACs, PACs, cosmids of the intervals.
- Task 3: Months 14-20: Perform FISH to confirm that the large physical clones map to the interval of interest. Make a plasmid library, screen for single copy clones, sequence, and design primers to map new markers on somatic cell hybrid panels to the critical interval.
- Task 4: Months 1-30: construct hybrid cell lines from lymphoblasts of newly identified deletion patients; delineate the extent of the deletions by genotyping of regional markers on hybrid lines.
- Task 5: Months 20-36: determine if there is a correlation between deletion extent and age of onset of neurofibromas; write a manuscript of study results; assess whether an *NF1* gene dosage PCR assay or FISH assay to detect deletion of the critical region has sufficient predictive value to warrant development of a diagnostic test.

a. [Tasks 1 & 2]. In collaboration with Dr. Anthony Harmar's laboratory, we have mapped the serotonin transporter (SLC6A4) and the carboxypeptidase D (CPD1) genes to the marker region 5, which is just centromeric to the cenBCR. These 2 genes are deleted in patient UWA106-3#36 who carries the largest microdeletion identified to date. Because these genes are not deleted in 16 other unrelated microdeletion patients, it is unlikely that their haploinsufficiency contributes to the early onset of neurofibromas.

Details of this research are in the attached manuscript:

Shen S, Battersby S, Weaver M, Clark E, Stephens K, Harmar AJ. Refined mapping of the human serotonin transporter (SLC6A4) gene within 17q11 adjacent to the CPD and *NF1* genes. *Eur J Hum Genet*, in press.

b. [Tasks 1, 2, 4]. To validate our manual gene dosage assay, 30 patients with early onset neurofibromas, atypical facial features, mental retardation, and/or other findings suggestive of a contiguous gene deletion were screened (Table 1, below). The assay predicted that 21 patients were disomic at *NF1*, 6 monosomic at *NF1*, and 3 were of "intermediate" *NF1* zygosity. Fluorescent *in situ* hybridization and somatic cell hybrid analyses provided physical confirmation that the 6 apparent monosomic patients were deleted for about 1- 2 Mb, which spanned an entire *NF1* allele and contiguous flanking regions. All of the centromeric and telomeric microdeletion breakpoints were clustered in two discrete marker intervals. The centromeric breakpoints mapped between D17S1294 and UT172, while the telomeric deletion breakpoints mapped between D17S1800 and D17S798. These data suggest the presence of recombination-prone sequences that flank the *NF1* locus. The development and application of PCR-based gene dosage assays for loci across a deleted region will provide rapid identification and genotyping of patients with microdeletions for detection of genotype/phenotype correlations.

A manuscript detailing these results was submitted. The reviewers requested additional clinical information on the new deletion patients. After considerable efforts to obtain, this information is now being incorporated into the revised manuscript. K. Maruyama, M. Weaver, K.A. Leppig, R. Farber, A. Aylsworth, Michael Dorschner, J. Ortenberg, A. Rubenstein, L. Immken, E. Haan, C. Curry and K. Stephens. Quantitative PCR gene dosage assay for detection of NF1 contiguous gene deletions. Submitted, in revision.

c. [Tasks 1,3,4,5]. We have constructed a 3.5 Mb BAC/PAC/YAC contig at chromosome 17q11.2 (Figure 4). Analysis of somatic cell hybrids from microdeletion patients showed that 14 of 17 cases had deletions of 1.5 Mb in length. The deletions encompassed the entire 350 kb NF1 gene, 3 additional genes, 1 pseudogene and 16 ESTs. In these cases, both proximal and distal breakpoints mapped at chromosomal regions of high identity, termed NF1REPs. These REPs, or clusters of paralogous loci, are 15-100 kb and harbor at least 4 ESTs and an expressed SH3GL pseudogene. (Figure 5). The remaining 3 patients had at least one breakpoint outside of an NF1REP element; one had a smaller deletion thereby narrowing the critical region harboring the putative locus that exacerbates neurofibroma development to 1 Mb. The physical features of the 13 unrelated NF1 microdeletion patients and the 4 members of family UWA166 are summarized (Table 2). There were no obvious differences detected between the features present in those individuals with the common NF1 deletion and the three with deletions of different lengths. No single feature was present or absent consistently within either group. The location of the putative gene that potentiates neurofibromagenesis was narrowed to an interval of 1 Mb between FB12A2 and SH3GLP1, as defined by the deletion of patient UWA113-1 (Figure 4). This critical region is known to harbor 4 genes, 2 pseudogenes, and 7 ESTs (Figure 4). Together, these data indicate that the likely mechanism of NF1 microdeletion is homologous recombination between NF1REPs on sister chromatids.

NF1 microdeletion is the first REP-mediated rearrangement identified that results in loss of a tumor suppressor gene. Therefore, in addition to the germline rearrangements reported here, NF1REP-mediated somatic recombination could be an important mechanism for the loss of heterozygosity (LOH) at *NF1* in tumors of NF1 patients. In fact, we hypothesize that the somatic deletions leading to LOH in leukemic cells of a subset of NF1 patients (see below) may arise by REP-mediated recombination. As detailed in the attached manuscript, these data have broad applications to the mechanisms of somatic rearrangements during neoplasia.

A manuscript detailing this work is in the appendix. It was provisionally accepted by Human Molecular Genetics journal pending minor revisions, which have been made. Dorschner MO, Sybert VP, Weaver M, Pletcher BA, Stephens K. NF1 microdeletion breakpoints are clustered at flanking repetitive sequences. Hum Mol Genet, submitted.

Therefore, Objective 2 is nearly complete. We are currently defining the length of the NF1-REPs, determining if there is a recombination hotspot, and mapping the novel recombination breakpoints. We hypothesize that these breakpoints occurred at regions that have "partial" NF1REP sequences. In addition, we plan to map the novel deletions of any additional patients that are identified in Objective 1.

Table 1. Results of screening patients for deletions using the NF1 gene dosage assay.

No. Patients		Findings present in patients of each phenotypic class ¹					No. of patients with NF1 zygosity as predicted by the gene dosage assay ²		
		NF1 diagnostic criteria fulfilled ³	Additional findings ⁴	Facial anomalies	Sporadic NF1	Familial NF1			
Screened	Class						Disomic	Intermediate	Monosomic
13	A	+		+	+		8	2	3
4	B	+		+		+	4	0	0
6	C	+	+	+/-	+		2	1	3
7	D	-	+/-	+	+		7	0	0
Total	30						21	3	6

10-A

¹Feature(s) present (+) or absent (-) in all patients in the category; (+/-) present in some patients in the category.

²NF1 gene dosage values for disomy (0.82 - 1.14), monosomy (0.37 - 0.53), and intermediate (0.54- 0.81).

³Diagnostic criteria from NIH Consensus Development Conference, 1988. Patients in category D were less than 6 years of age and had presumptive NF1 based primarily on presence of café au lait spots.

⁴One or more of documented mental retardation, abnormal CNS findings, multiple congenital anomalies, dramatically excessive tumor burden, additional findings consistent with a second genetic disorder, or malignancy at less than age 25.

Legends for Figures below:

Figure 4. Physical contig of the *NF1* region. The thick black bar is a schematic of the chromosome 17q11.2 region with STS loci placed above the bar and genes and EST loci below. The BAC, PAC, and YAC clones comprising the contig are shown above; open ellipses are aligned with the loci on the chromosome schematic and indicate a positive hit in the clone; sequenced BAC/PAC clones are indicated with an asterisk. Vertical bars at the ends of BACs represent insert termini that were sequenced and submitted to Genbank, but not converted to amplimers. Scale in Mb is at the top of the figure. The size and extent of microdeletions of NF1 patients are shown below the chromosome. The common *NF1* deletion region was identified in 14 out of 17 unrelated patients; while 3 patients had novel deletions as shown. The open boxes represent flanking repetitive sequences (NF1REP) where the majority of breakpoints mapped.

Figure 5. NF1REP domains on chromosome 17. The locations of the three NF1REP regions, designated -P, -M, -D for proximal, medial, and distal are shown along with the 5 loci they are known to contain. In addition, the closest unique marker flanking each REP is indicated. The cross-hatched bar represents the 1.5 Mb region commonly deleted in *NF1* microdeletion patients.

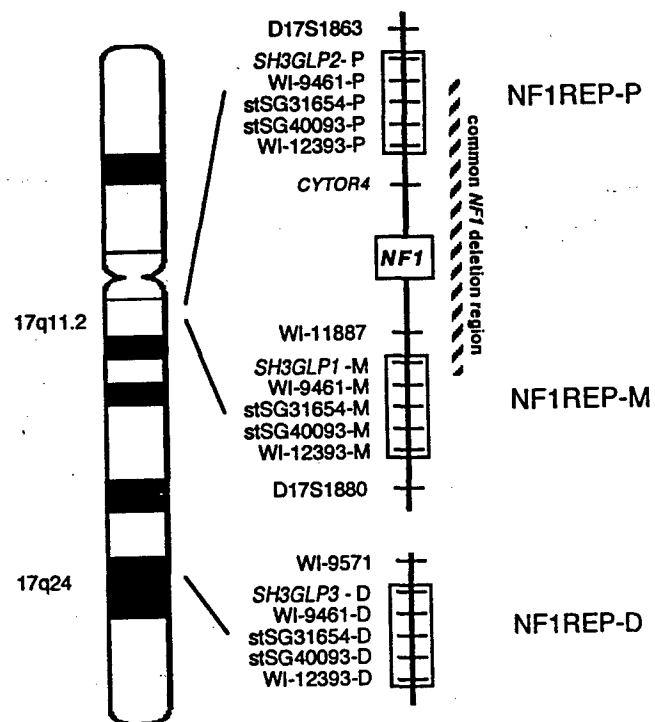


Figure 5

Table 2-1 Physical features of subjects with *NF1* microdeletions

Patient ID ¹	Cutaneous neurofibromas ²		Ht ³	Macrocephaly (cm)	Facial Features	Intelligence ⁴	Hands / Feet	Heart ⁵	Other Tumors	
	Age	Number							Type, Number	Age
Patients with deletion breakpoints at NF1REP-P and NF1REP-M										
69-3	8	many	5%	-(54.5)	hypertelorism	IQ 59	"normal"		plexiform neurofibroma, 2	10
119-1	22	TNTC	50%	+	hypertelorism	IQ 80s "dull normal"	NI	-		
123-3	5	many	Nml	+	hypertelorism, Ptosis	LD	25-50%	ASD	plexiform neurofibroma, 1 neurofibrosarcoma, 1	5 9
128-3	7 29	Several TNTC	3%	-(55)	Ptosis, downslanting palpebral fissures	normal	10-25%	-		
147-3	6	numerous	40%	-	Hypertelorism, ptosis, coarse, downslanting palpebral fissures	significant delays	NI	-		
156-1	31	TNTC	NI	NI	"dysmorphic"	mild MR with severe LD	NI	-	optic glioma	
160-1	11 35	Several TNTC	<3%	NI	"Noonan-like," coarse	LD, special education	NI	-	plexiform neurofibroma, 1	7
166-1	39	TNTC	NI	NI	telecanthus, downslanting palpebral fissures	"dull"	"large"	-		
166-2	7 19	Several TNTC	90%	-(56.5)	hypertelorism, downslanting palpebral fissures	special education	>97%	-		
166-3	4	none	NI	-(49)	downslanting palpebral fissures, "unusual face"	"normal", speech impediment	97%	-		
166-4	5 6	none 9	90%	-(48.5)	downslanting palpebral fissures	"normal", speech problems	97%	-		
167-1	4 7	7 20	NI	NI	ptosis, broad neck	mild development delay	NI	ASD, PS		

Table 2-2 Physical features of subjects with NF1 microdeletions

169-1	18	present	NI	+	coarse, hypertelorism, downslanting palpebral fissures	"dull normal," LD	"large"	Dilated aortic valve replaced	see footnote ⁶
172-1	childhood	None	NI	NI	"dysmorphic"	severe LD	"large"	-	optic glioma, 1 plexiform neurofibroma, 2
176-1	35	TNTC	NI	-	webbed neck, "Noonan"	WISC-III, mild/borderline MR	97%	-	plexiform neurofibroma, 2
183-1	12	10	25-50%	NI	hypertelorism, ptosis, broad nose	borderline development delay	50%	PS	plexiform neurofibroma, 1
184-1	5	TNTC	NI	NI	telecanthus, coarse face	IQ 71 fullscale, 81 verbal, 66 performance	97%	-	

Patients with at least one unique *NF1* deletion breakpoint

106-3	18	TNTC	Nml	+	(61.5)	coarse	IQ 46	"large"	-	plexiform neurofibroma, 1 spinal neurofibromas, TNTC	3
113-1	8	TNTC	10%	+	(59)	coarse, hypertelorism	IQ 88 LD	>97%	-	-	25
155-1	15	TNTC	NI	+	(59.5)	coarse, ptosis	moderate MR	>97% hands 75% feet	-	spinal neurofibroma, 1 neurofibrosarcoma, 1	sym 27
	27	TNTC	NI	+	(59.5)	coarse, ptosis			-	see footnote ⁷	28

¹The UWA- prefix for patient identifiers is not shown. All patients are unrelated, with the exception of 4 members of family UWA166.²Age in years; TNTC, too numerous to count.³Height in percentile; Nml, normal; NI, no information available.⁴LD, learning disabilities; MR, mental retardation.⁵PS, pulmonic stenosis; ASD, atrial septal defect.⁶Patient's mother and sister with NF1, presumably due to the same NF1 microdeletion, had retroperitoneal fibrosarcoma with metastases (~age 30) and cerebellar medulloblastoma (age 16), respectively.⁷Spinal neurofibroma was symptomatic at age 27; patient inherited NF1 from his father who died of malignant CNS tumor in 5th decade.

C. Technical Objective 3: To determine if somatic uniparental disomy (UPD) of the *NF1* region is a frequent event in leukemic tumor tissue and to investigate somatic mechanisms of uniparental disomy.

Task 1: Months 1-12: obtain additional tumor samples and determine their *NF1* gene dosage by the gene dosage PCR assay; confirm by *NF1* FISH that tumors predicted to undergo LOH by UPD have two *NF1* alleles, while those predicted to result from LOH by deletion have one *NF1* allele; determine the frequency of UPD-LOH.

Task 2: Months 10-25: Map the extent of each uniparental disomy region; assay normal tissue for mosaicism for the UPD of the *NF1* region; write a manuscript addressing mechanisms of UPD-LOH.

This Objective 3 is nearly completed and two manuscripts are currently being written. Because the results of this study were so remarkable and novel, we decided to focus on this aim earlier during the study period than was anticipated in the original Statement of Work.

a. The patterns of LOH at chromosome 17 loci were analyzed to gain insight into the mechanisms leading to allelic loss of *NF1* in primary leukemia cells of *NF1* children. Analysis of bone marrows by gene dosage PCR and interphase FISH from 11 unselected cases (Tables 3 and 4) showed that LOH occurred by two distinct mechanisms, each of which resulted in loss of the normal *NF1* allele. Three tumors (30%) had interstitial microdeletions between D17S1294 and D17S250, an estimated distance of 22 cM or 17 Mb that spanned the normal *NF1* gene at chromosome 17q11.2 (Figure 6). The remaining 8 cases (70%) resulted from isodisomy for a 50 Mb chromosomal segment harboring a defective *NF1* allele. In at least 4 of these cases, the isodisomic segment was interstitial to the chromosome 17q arm and estimated to be 55 Mb in length.

This is the first report of interstitial isodisomy at common breakpoints as a mechanism of LOH (Table 5). We propose that interstitial isodisomy arose by a double mitotic recombination event between non-sister chromatids during the S/G2 phase of the cell cycle of an ancestral cell. Remarkably, the isodisomic breakpoints in all 8 cases examined were in a 2.7 cM centromeric interval between D17S959 and D1294, an estimated physical length of 5.3 Mb. The telomeric breakpoints in 4 cases mapped to a 9.6 cM interval flanked by D17S1822/D17S1830 and D17S928, an estimated physical length of 7.2 Mb. The clustering of the both LOH breakpoints suggests the existence of recombination-prone sequences in these regions of chromosome 17. While functional inactivation of neurofibromin is apparently sufficient for the myeloproliferative phenotype, these data suggest a putative role of modifying locus on chromosome 17 that may contribute to the development of leukemia. This locus may in fact be low copy number repeat sequences and/or sites that predispose to chromosome breakage, which together facilitate the double mitotic recombination events leading to LOH.

A manuscript detailing this work is currently being written. Karen Stephens, Molly Weaver, Kathy Leppig, Kyoko Maruyama, Elizabeth M. Davis, Rafael Espinosa, III, Melvin H. Freedman, Peter Emanuel, Lucy Side, Michelle M. Le Beau, Kevin Shannon. Tumor suppressor inactivation by double mitotic recombination at clustered breakpoint intervals. In preparation.

Table 3. NF1 gene dosage in bone marrows of NF1 children with malignant myeloid disorders.

Patient No.	Sex	Age at Onset	Diagnosis	Origin of NF1 mutation	LOH at NF1 Locus	NF1 Gene Dosage Value ^{a,b}	Predicted NF1 Gene Copy No. ^a
1	M	9 mo	MPS	<i>de novo</i> (paternal)	maternal	0.99	disomy
2	M	10 mo	AML	paternal	maternal	0.93	disomy
3	M	24 mo	monosomy 7	unknown	maternal	0.96	disomy
4	M	14 mo	JMML	maternal	paternal	0.86	disomy
5	F	30 mo	JMML	maternal	paternal	0.94	disomy
6	M	10 mo	JMML	maternal	paternal	0.87	disomy
7	M	5 mo	monosomy 7	maternal	paternal	0.90	disomy
8	F	18 mo	MPS	paternal	maternal ^a	0.85	disomy
9	M	5 yr	JMML	maternal	paternal	0.57	monosomy
10	M	19 mo	monosomy 7	<i>de novo</i>	maternal ^a	0.48	monosomy
11	F	18 mo	JMML	unknown	probable	0.44	monosomy

^aData from this manuscript.

^bMeasured in unfractionated bone marrow cells, except patients 3, 9 for whom leukemic cells in peripheral blood were used.

Table 4. Interphase fluorescence *in situ* hybridization analysis of bone marrow samples.

Patient	Chr. 17	Number of Hybridization Signals					Control	Number of Hybridization				
		0	1	2	3	≥4		0	1	2	3	≥4
3	Cep®1	0	6	87	3	4						
	P1-9	0.6	14	84	1	0.4	263P1	0		90	2	0.4
	P1-12	1	13	80	6	0	263P1	0	9	88	2	1
3	P1-9	4	4	92	0	0	Cep®7	0	92	8	0	0
	P1-12	2	4	94	0	0	Cep®7	0	89	11	0	0
4	Cep®1	0	5	90	2	3						
	P1-9	0.5	10	86	3	0.5	263P1	0	12	84	2	1.5
	P1-12	0.5	13	78	8	0/5	263P1	0.4	7	92	0.6	0
5	Cep®1	0	6	93	0	1						
	P1-9	6	7	82	4	1	263P1	1	4	90	4	1
	P1-12	0.4	6	90	2.6	1	263P1	0.2		93	0.5	1.5
6	Cep®1	0	2	97	1	0						
	P1-9	1	5	95	0	0	263P1	0	25	74	1	0
	P1-12	1	9	76	12	2	263P1	0	15	84	0	1
10	Cep®1	0.8	3.6	95	0.6	0						
	P1-12	4	29	67	0	0	263P1	0	3	97	0	0
C1	Cep®1	0	6.4	93	0.6	0						
	P1-9	3	7	89	1	0	263P1	2	3	86	5	4
	P1-12	2	5	89	2	2	263P1	0	7	90	1.5	1.5
C2	Cep®1	1	3	95	1	0						
	P1-9	2	22	76	0	0	263P1	1	19	79	1	0
	P1-12	0.5	7	86	5	1.5	263P1	1.6	6	88	3	1.4
C3	Cep®1	0	5	94	0	0						
	P1-9	1.5	12	81	4	1.5	263P1	0	8	90	2	0
	P1-12	0	9	85	3.4	2.6	263P1	0	8	89	2	1
C4	Cep®1	0	4	96	0	0						
	P1-9	0.5	11	83	1.5	2	263P1	0.5	9	88	2	0.5
	P1-12	0.5	9.5	85	4	1	263P1	0.5	17	82	0.5	0
C5	Cep®1	0	6	93	1	0						
	P1-9	1	6	92	0.5	0.5	263P1	0.6	4	95	0.2	0.2
	P1-12	0	5	94	1	0	263P1	0	3	96	0.8	0.2
¹ Controls N=10	Cep®1											
	Mean	0.15	4.5	95	0.24	0.15						
	S.D.	0.19	0.79	0.83	0.25	0.16						

*Probe 263P1 is a 70 kb PAC clone containing D5S479 (chromosome band 5q31 ; Cep®17 and Cep®7 are centromere-specific probe for chromosomes 17 and 7, respectively. Patients no. 3-6 are described in Table 1. C1

is a cryopreserved bone marrow sample from a patient with AML-M4 in complete remission. C2-C5 are cryopreserved bone marrow samples from 4 children with myeloid leukemias that retained heterozygosity at the *NFI* locus. [†]The distribution of signals for the chromosome 17 centromere-specific probe was determined by the interphase analysis of bone marrow cells from 10 healthy individuals.

Figure 6

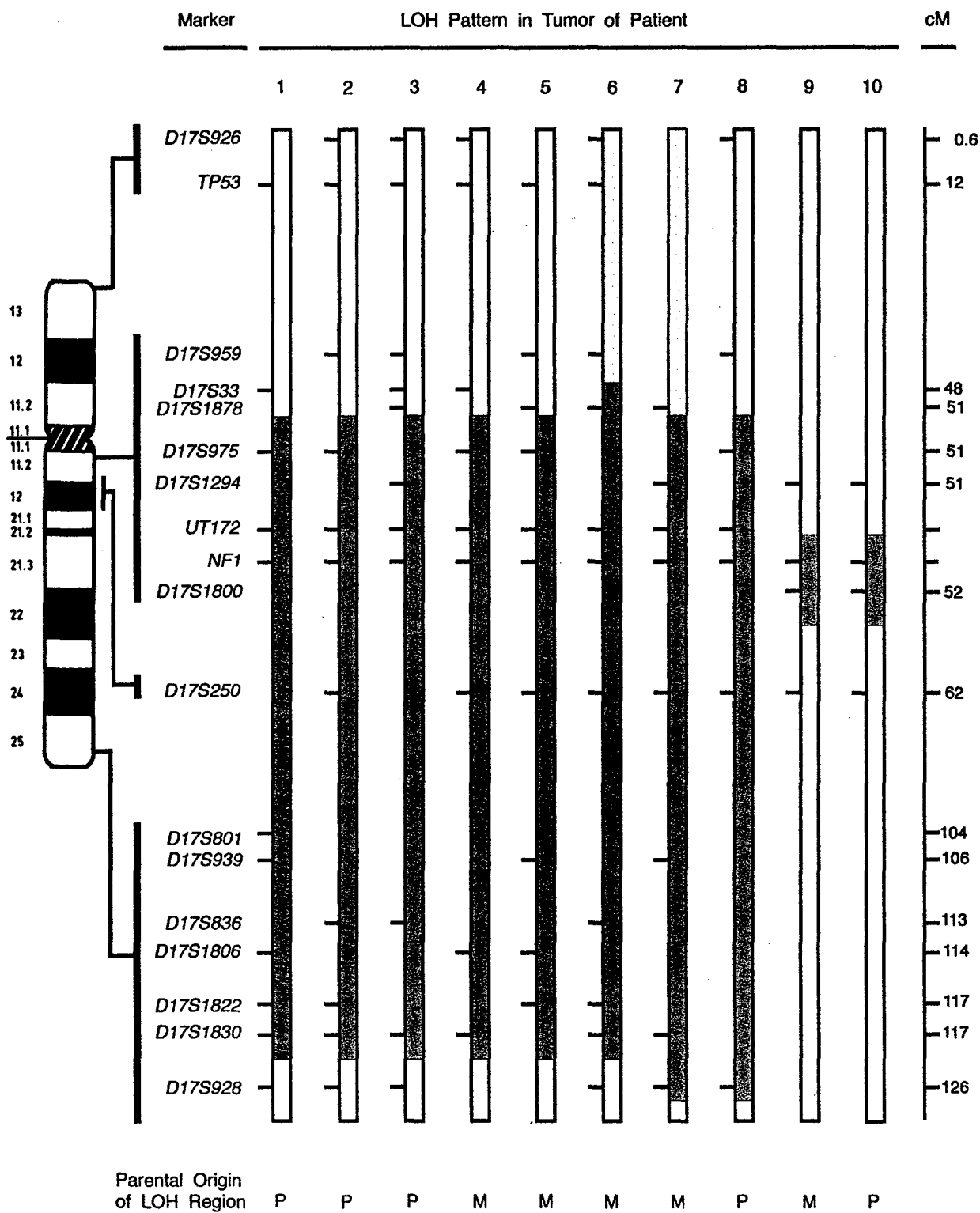


Figure 6 . Identical chromosome 17 loci showed LOH in both primary leukemic and lymphoma cells. The bars represent a schematic of the patient's paternally-derived chromosome 17 in specific tissues tested. Loci that showed LOH are in the shaded regions, while loci that retained heterozygosity are in the open regions. The location of loci are depicted on the chromosome ideogram with interlocus genetic distances in centiMorgans (cM) to the left of each interval as estimated from a chromosome 17 sex-averaged map (<http://www.marshmed.org/genetics/>). Data illustrating the retention of heterozygosity at the D17S805 locus and the loss of heterozygosity at the D17S1294 locus are shown to the right. DNA samples are lane 1, patient's unaffected father; lane 2, patient's mother affected with NF1; lane 3, patient's unfractionated bone marrow; lane 4, patient's unfractionated lymph node; lane 5, CD3-positive cells from the lymph node; lane 6, CD4-positive cells from the lymph node; positive and negative controls are not shown. For each locus, two alleles designated simply as A and B are segregating in this family.

Table 5. Genetic mechanisms leading to somatic inactivation of tumor suppressor genes^a.

Constitutional heterozygosity at tumor suppressor	LOST		RETAINED
Tumor Genotype	Hemizygous (monosomic)	Homozygous (Disomic)	Heterozygous
Single Locus Affected	<ul style="list-style-type: none"> • intragenic deletion • illegitimate V(D)J recombination 	<ul style="list-style-type: none"> • gene conversion 	<ul style="list-style-type: none"> • compound heterozygous mutations • methylation → transcriptional silencing
Multiple Loci Affected	<ul style="list-style-type: none"> • multilocus deletion • nondisjunction → chromosome loss • unbalanced chromosome abnormalities → e.g., translocation, isochromosome 	<ul style="list-style-type: none"> • nondisjunction, chromosome loss, reduplication → chromosomal isodisomy • single homologous recombination → partial isodisomy • double homologous recombination → interstitial isodisomy 	

b. We have also mapped the LOH region in different tissues from a child with juvenile monomyelocytic leukemia (JMML), who later developed a T cell lymphoma. We have demonstrated that the mechanism of LOH was by an interstitial deletion and that the LOH regions were identical in length in the B cells, lymph node, and sorted cells from the node (Figure 7). These data show that the malignant JMML and lymphoid cells shared a common loss of genetic material involving the NF1 gene, suggesting that the abnormal T lymphoid and myeloid populations were derived from a common cell. These data support the hypothesis that JMML can arise in a pluripotent hematopoietic cell.

A manuscript detailing this work is currently being written. Cooper LJN, Shannon KM, Loken M, Weaver M, Stephens K, Sievers EL. Evidence that juvenile myelomonocytic leukemia can arise from a pluripotential stem cell. In preparation.

LOH in Patient Tissues

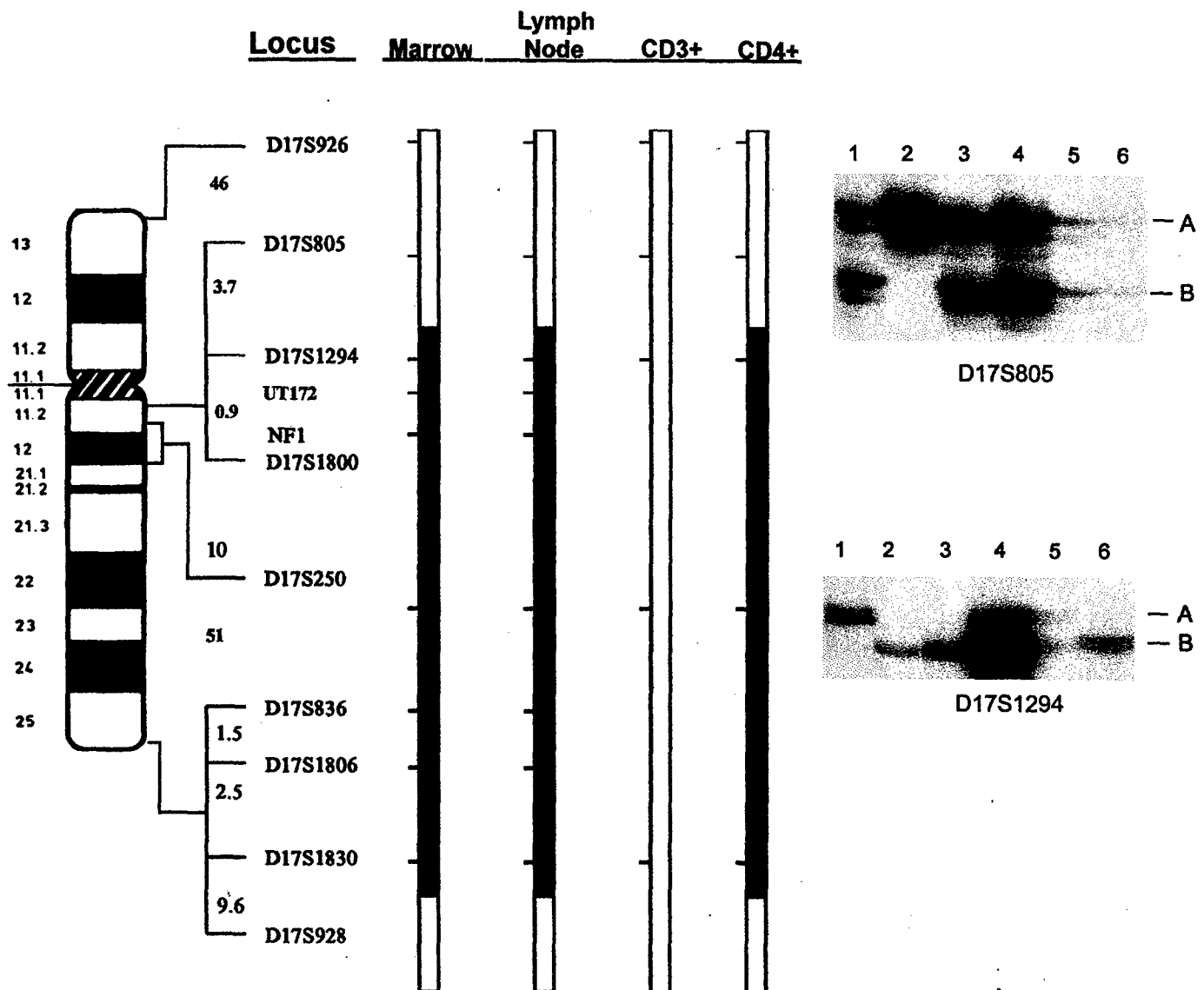


Figure 7. Identical chromosome 17 loci showed LOH in both primary leukemic and lymphoma cells. The bars represent a schematic of the patient's paternally-derived chromosome 17 in specific tissues tested. Loci that showed LOH are in the shaded regions, while loci that retained heterozygosity are in the open regions. The location of loci are depicted on the chromosome ideogram with interlocus genetic distances in centiMorgans (cM) to the left of each interval as estimated from a chromosome 17 sex-averaged map (<http://www.marshmed.org/genetics/>). Data illustrating the retention of heterozygosity at the D17S805 locus and the loss of heterozygosity at the D17S1294 locus are shown to the right. DNA samples are lane 1, patient's unaffected father; lane 2, patient's mother affected with NF1; lane 3, patient's unfractionated bone marrow; lane 4, patient's unfractionated lymph node; lane 5, CD3-positive cells from the lymph node; lane 6, CD4-positive cells from the lymph node; positive and negative controls are not shown. For each locus, two alleles designated simply as A and B are segregating in this family.

7. Key Research Accomplishments

- designing and validating an automated PCR-based gene dosage assay that can be readily adapted to any unique locus in the genome
- constructing a detailed 3.5 Mb physical map of the NF1 gene region at 17q11.2
- identifying recombination-prone repeat sequences (NF1REPs) that flank the NF1 gene and that they are comprised of clusters of paralogous loci
- proving that NF1 microdeletions arise by recombination between paralogous regions (NF1REPs)
- proving that NF1 microdeletion is the first reported REP-mediated rearrangement that deletes a tumor suppressor gene. This has broad implications for molecular mechanisms that cause neoplasia
- proving that loss of heterozygosity in leukemic cells of children with NF1 primarily occurs by the novel mechanism of a double mitotic recombination event at clustered sites
- demonstrating that JMML can arise in a pluripotent hematopoietic cell.

8. Reportable Outcomes

- Manuscripts

Shen S, Battersby S, Weaver M, Clark E, Stephens K, Harmar AJ. Refined mapping of the human serotonin transporter (SLC6A4) gene within 17q11 adjacent to the CPD and NF1 genes. *Eur J Hum Genet*, in press.

Dorschner MO, Sybert VP, Weaver M, Pletcher BA, Stephens K. NF1 microdeletion breakpoints are clustered at flanking repetitive sequences. *Hum Mol Genet*, submitted.

Maruyama, M. Weaver, K.A. Leppig, R. Farber, A. Aylsworth, Michael Dorschner, J. Ortenberg, A. Rubenstein, L. Immken, E. Haan, C. Curry and K. Stephens. Quantitative PCR gene dosage assay for detection of NF1 contiguous gene deletions. Submitted, in revision.

Karen Stephens, Molly Weaver, Kathy Leppig, Kyoko Maruyama, Elizabeth M. Davis, Rafael Espinosa, III, Melvin H. Freedman, Peter Emanuel, Lucy Side, Michelle M. Le Beau, Kevin Shannon. Tumor suppressor inactivation by double mitotic recombination at clustered breakpoint intervals. In preparation.

Cooper LJN, Shannon KM, Loken M, Weaver M, Stephens K, Sievers EL. Evidence that juvenile myelomonocytic leukemia can arise from a pluripotential stem cell. In preparation.

- Abstracts

Stephens K, Weaver M, Leppig K, Maruyama K, Side L, Davis EA, Espinosa III R, Le Beau M, Shannon K. 1998. Double mitotic recombination at common breakpoint intervals leading to interstitial isodisomy and LOH. *Am J Hum Genet* 63(4): A205.

Dorschner MO, Weaver M, Sybert VP and Stephens K. 1999. NF1 microdeletions are mediated by homologous recombination between duplicons. *Am J Hum Genet* 65(4): A151.

Stephens K, Weaver M, Leppig K, Maruyama K, Side L, Davis EA, Espinosa III, R, Le Beau M, and Shannon K. A novel and frequent mechanism of loss of heterozygosity in malignant myeloid cells of NF1 children: Double mitotic recombination at common breakpoint intervals. National Neurofibromatosis Foundation Consortium, June, 1998, Aspen, CO.

- Presentations

K. Stephens. A novel and frequent mechanism of loss of heterozygosity in malignant myeloid cells of NF1 children? Double mitotic recombination at common breakpoint intervals. American Society of Human Genetics, October, 1998, Denver.

M. Dorschner. NF1 microdeletions are mediated by homologous recombination between duplicons. American Society of Human Genetics, October, 1999, San Francisco.

K. Stephens. A novel and frequent mechanism of loss of heterozygosity in malignant myeloid cells of NF1 children: Double mitotic recombination at common breakpoint intervals. National Neurofibromatosis Foundation Consortium, June, 1998, Aspen, CO.

K. Stephens. Progress on NF1 research at the University of Washington. Washington Chapter, National Neurofibromatosis Foundation, February, 1998. Invited speaker.

- **Invited participant at meetings.**

National Neurofibromatosis Foundation International Consortium on Gene Cloning and Gene Function of NF1 and NF2, Boston, 1999

- **Databases**

We developed a database in FileMaker Pro to track all of the NF1 patients referred for this research study. Fields clinical history, referring physician, tissue available for study, etc.

We developed a database in FreezerWorks to track the multiple vials of immortalized patient cells that are stored in a liquid nitrogen freezer.

- **Cell lines**

We have established immortalized lymphoblastoid cell lines for approximately 20 patients and relatives. In addition, we constructed somatic cell hybrids carrying each of a patient's chromosome 17s for 5 cases.

- **Funding applied for**

Genetic factors that affect tumorigenesis in NF1.

Principal Investigator: Karen G. Stephens

Submitted to U.S. Army Medical Research and Materiel Command

1. Conclusions

We have determined that very unusual rearrangements involving the NF1 gene occur in both germline and somatic tissues of certain patients. Germline microdeletions of 1.5 Mb are caused by recombination between repeated elements that flank the NF1 gene. Identification of these elements suggests that perhaps a subset of individuals are prone to de novo NF1 microdeletion due to individual variation in size, number, or complexity of these repeats. Our data provide strong support for a co-deletion of NF1 and a novel gene that potentiates neurofibromagenesis and narrow the chromosomal region of this putative gene to 1Mb. We describe the larger number and most detailed clinical description of NF1 deletion patients to date; these data suggest that NF1 microdeletion may be predictive for an early age at onset and large numbers of cutaneous neurofibromas. We have developed an automated PCR-based gene dosage assay to rapidly identify and map the extent of NF1 deletions. This assay will facilitate further research and should be directly applicable to diagnostic testing of patients for NF1 deletion. We describe for the first time somatic rearrangements tumor cells that arise by double mitotic recombination with clustered breakpoints. These rearrangements result in interstitial isodisomy for a 50 Mb region of chromosome 17 and occurred in leukemic tumor cells of children with NF1 and myeloid dysplasia. Because both the germline and somatic rearrangements involve not only the NF1 gene but many other genes, our data implicate other

elements/loci that play an important role in sporadic cases of NF1 and in somatic loss of NF1 during leukemogenesis and possibly during other NF1-associated neoplasias. In addition, these results have direct implications for rationale design of putative therapies.

10. References

- Kayes, L. M., Burke, W., Riccardi, V. M., Bennett, R., Ehrlich, P., Rubenstein, A., and Stephens, K. (1994) Deletions spanning the neurofibromatosis 1 gene: identification and phenotype of five patients. *Am J Hum Genet* 54:424-36.
- Kayes, L. M., Riccardi, V. M., Burke, W., Bennett, R. L., and Stephens, K. (1992) Large de novo DNA deletion in a patient with sporadic neurofibromatosis 1, mental retardation, and dysmorphism. *J Med Genet* 29:686-90.
- Leppig, K., Kaplan, P., Viskochil, D., Weaver, M., Orterberg, J., and Stephens, K. (1997) Familial neurofibromatosis 1 gene deletions: cosegregation with distinctive facial features and early onset of cutaneous neurofibromas. *Am J Med Genet* 73:197-204.
- Leppig, K. A., Viskochil, D., Neil, S., Rubenstein, A., Johnson, V. P., Zhu, X. L., Brothman, A. R., and Stephens, K. (1996) The detection of contiguous gene deletions at the neurofibromatosis 1 locus with fluorescence in situ hybridization. *Cytogenet Cell Genet* 72:95-8.
- Miles, D., Freedman, M., Stephens, K., Pallavicini, M., Sievers, E., Weaver, M., Grunberger, T., Thompson, P., and Shannon, K. (1997) Patterns of hematopoietic lineage involvement in children with neurofibromatosis, type 1 and malignant myeloid disorders. *Blood* 88:4314-4320.
- Mulvihill, J. J. (1994) Malignancy: epidemiologically associated cancers. In: (S. M. Huson, and R. A. C. Hughes, eds.) *The Neurofibromatoses: A pathogenetic and Clinical Overview*. Chapman & Hall Medical, London, pp. 487.
- Riccardi, V. M. (1993) Molecular biology of the neurofibromatoses. *Semin Dermatol* 12:266-73.
- Shannon, K. M., P. O. C., Martin, G. A., Paderanga, D., Olson, K., Dinndorf, P., and McCormick, F. (1994) Loss of the normal NF1 allele from the bone marrow of children with type 1 neurofibromatosis and malignant myeloid disorders. *N Engl J Med* 330:597-601.
- Wu, B. L., Schneider, G. H., and Korf, B. R. (1997) Deletion of the entire NF1 gene causing distinct manifestations in a family. *Am J Med Genet* 69:98-101.
- Wu, B.-L., Austin, M., Schneider, G., Boles, R., and Korf, B. (1995) Deletion of the entire NF1 gene detected by FISH: four deletion patients associated with severe manifestations. *Am J Med Genet* 59:528-535.

11. Appendices

Stephens K, Weaver M, Leppig K, Maruyama K, Side L, Davis EA, Espinosa III R, Le Beau M, Shannon K. 1998. Double mitotic recombination at common breakpoint intervals leading to interstitial isodisomy and LOH. *Am J Hum Genet* 63(4): A205.

Dorschner MO, Weaver M, Sybert VP and Stephens K. 1999. NF1 microdeletions are mediated by homologous recombination between duplicons. *Am J Hum Genet* 65(4): A151.

Stephens K, Weaver M, Leppig K, Maruyama K, Side L, Davis EA, Espinosa III, R, Le Beau M, and Shannon K. A novel and frequent mechanism of loss of heterozygosity in malignant nyeloid cells of NF1 children: Double mitotic recombination at common breakpoint intervals. National Neurofibromatosis Foundation Consortium, June, 1998, Aspen, CO.

Shen S, Battersby S, Weaver M, Clark E, Stephens K, Harmar AJ. Refined mapping of the human serotonin transporter (SLC6A4) gene within 17q11 adjacent to the CPD and NF1 genes. Eur J Hum Genet, in press.

Dorschner MO, Sybert VP, Weaver M, Pletcher BA, Stephens K. NF1 microdeletion breakpoints are clustered at flanking repetitive sequences. Hum Mol Genet, submitted.

√ The following abstract is submitted for oral presentation or poster presentation

ABSTRACT

A novel and frequent mechanism of loss of heterozygosity in malignant myeloid cells of NF1 children: Double mitotic recombination at common breakpoint intervals

K Stephens¹, M Weaver¹, K Leppig¹, K Maruyama¹, L Side³, EA Davis², R Espinosa III²,
M Le Beau², K Shannon³

¹University of Washington, ²University of Chicago, ³University of California, San Francisco
¹Depts Medicine and Laboratory Medicine, Mail Box 357720, University of Washington, Seattle, WA
98195

Ph 206-543-8285; Fax 206-685-4829, millie@u.washington.edu

Leukemic cells of NF1 children with malignant myeloid disorders commonly show loss of constitutional heterozygosity (LOH) at the NF1 gene and flanking loci. We have found that a novel mechanism of LOH is employed, which involves an apparent double mitotic recombination at common breakpoint intervals. Quantitative PCR and FISH analyses of leukemic cells revealed that, despite showing LOH at NF1, these cells harbor two NF1 alleles. NF1 LOH in conjunction with NF1 disomy was detected in 9 out of 11 cases analyzed. Six of these cases were further studied by genotypic analyses of loci spanning chromosome 17. In each of these 6 cases, a large interstitial region of the q arm of chromosome 17 showed LOH. The LOH breakpoints mapped to common intervals. The centromeric LOH breakpoint in 5 of 6 cases mapped centromeric to NF1 between D17S1878 and D17S975. The breakpoint of the remaining case mapped to an adjacent interval bounded by D17S1878 and D17S959. Similarly, 4 of the 6 cases had LOH breakpoints close to the telomere in intervals bounded by D17S928 and D17S1822/D17S1830. The other 2 cases had breakpoints within this region, but it is unclear if they map in the same interval due to lack of informative markers. Together, these data are consistent with a mechanism whereby the LOH region originated by a double mitotic recombination event in a hematopoietic progenitor cell that gave rise to the malignant clone. The high frequency of this rearrangement in leukemic cells of NF1 children implies that it either has biological significance, such as selecting for growth of the malignant clone, or is favored due to recombination-prone sequences in specific regions of chromosome 17.

Program Nr: 151

NF1 microdeletions are mediated by homologous recombination between duplicons. *M.O. Dorschner, M.A. Weaver, V.P. Sybert, K.G. Stephens.* Department of Medicine, University of Washington School of Medicine, Seattle, WA.

Neurofibromatosis type 1 patients with a submicroscopic deletion spanning the NF1 gene are remarkable for an early age at onset of cutaneous neurofibromas, suggesting the co-deletion of a novel locus that potentiates neurofibromagenesis. Construction of a 3.5 Mb BAC/PAC contig at chromosome 17q11.2 and analysis of somatic cell hybrids from microdeletion patients showed that 14 of 17 cases had deletions of 1.5 Mb in length. The deletions encompassed the entire 350 kb NF1 gene, 3 additional genes, 1 pseudogene, and 13 ESTs. The critical region harboring the putative locus that exacerbates neurofibroma development was narrowed to 1 Mb by the identification of a smaller deletion in one of the 3 remaining patients. Of the 14 cases with 1.5 Mb deletions, both the proximal and distal breakpoints mapped within chromosomal regions of high homology, termed NF1 duplicons. These duplicons, with an estimated length of 15-100 kb, harbor at least 4 ESTs and an expressed SH3GL pseudogene. Therefore, homologous recombination between duplicons either in cis or in trans on sister chromatids is a predominant mechanism of NF1 microdeletion. Refined breakpoint mapping will facilitate identifying sequences within the duplicons that are susceptible to chromosome breakage and recombination. The number of NF1 duplicons in the genome is unknown, however, we have identified a third one at chromosome 17q24. These data suggest that NF1 duplicons may also play a role in germline or somatic rearrangements other than those resulting in neurofibromatosis type 1.

AJHG 1998

Program Nr: 205

Double mitotic recombination at common breakpoint intervals leading to interstitial isodisomy and LOH. *K. Stephens¹; M. Weaver¹; K. Leppig¹; M. Maruyama¹; L. Side²; E. Davis³; R. Espinoza III²; M. Le Beau²; K. Shannon³* 1) Univ of Washington, Seattle, WA; 2) Univ of Chicago, Chicago, IL; 3) Univ of California, San Francisco, CA.

Leukemic cells of children with neurofibromatosis 1 (NF1) who develop malignant myeloid disorders commonly show loss of constitutional heterozygosity (LOH) of the normal NF1 allele at 17q11.2 and cytogenetically normal chromosomes 17. Mapping the LOH region revealed that the predominant mechanism is interstitial isodisomy. FISH and quantitative PCR analyses of 11 cases, whose bone marrows had LOH at the NF1 locus, showed that in 8 cases the leukemic cells were disomic for NF1, while the remaining 3 cases were monosomic. In each of the 8 NF1 disomic cases, a large interstitial 17q segment had undergone LOH with the breakpoints mapping to common intervals. The proximal LOH breakpoints mapped centromeric to NF1 between D17S1878 and D17S975, while the distal LOH breakpoints were subtelomeric and bounded by D17S928 and D17S1822/D17S1830. Together these data indicate that the leukemic cells were isodisomic for an ~50 Mb interstitial 17q segment which carried the mutated NF1 allele, thereby resulting in LOH and functional loss of NF1. Interstitial isodisomy most likely arose by a double mitotic recombination during the S/G2 cell cycle of a hematopoietic progenitor cell, which gave rise to the malignant clone. The high frequency and common recombination breakpoint intervals of these novel rearrangements imply that along with NF1, additional chromosome 17 loci play a role in development of malignant myeloid disorders in NF1 children, perhaps by favoring growth of the malignant clone. Because cases of maternal and paternal isodisomic regions were both observed, genomic imprinting is unlikely to be a factor. Bone marrow cells in the remaining 3 cases showed NF1 LOH, NF1 monosomy, and small LOH regions of 1-2 Mb spanning the NF1 locus, indicating that they arose by small interstitial deletions. These studies demonstrate that critical genetic loci and mechanisms underlying neoplasia may not be detected if LOH analyses are not performed in conjunction with physical mapping.

Refined mapping of the human serotonin transporter (SLC6A4) gene within 17q11
adjacent to the CPD and NF1 genes

Sanbing Shen^{*1}, Sharon Battersby¹, Molly Weaver², Elma Clark¹, Karen Stephens^{2,3} and
Anthony J. Harmar¹

¹MRC Brain Metabolism Unit, University Department of Neuroscience, 1 George
Square, Edinburgh EH8 9JZ, Scotland

Departments of ²Medicine and ³Laboratory Medicine, University of Washington, Seattle,
WA 98195

* corresponding author:
MRC Brain Metabolism Unit,
University Department of Neuroscience
1 George Square
Edinburgh
EH8 9JZ
Scotland

Tel: +44-131-537 6527
Fax: +44-131-537 6110

Email: sshen@srv1.bmu.mrc.ac.uk

Running Title: Mapping of the SLC6A4 gene adjacent to CPD and NF1

ABSTRACT

The SLC6A4 gene encodes the serotonin transporter, which is the target of an important class of antidepressant drugs, the serotonin selective reuptake inhibitors. Polymorphic variation in the SLC6A4 gene has been reported to be associated with susceptibility to depression and other psychiatric disorders. We have constructed a 1 Mb YAC and PAC contig which harbours both the SLC6A4 gene and the gene encoding carboxypeptidase D (CPD), a recently discovered membrane-bound metallocarboxypeptidase. The order of loci within the contig was cen-D17S975-D17S1549-24R-D17S1294-SLC6A4-28L-(CPD, D17S2009, D17S2004)-D17S2120-ter. Fluorescence in situ hybridisation and somatic cell hybrid analyses documented that both the SLC6A4 and CPD genes were deleted in 1 out of 17 neurofibromatosis type 1 (NF1) patients carrying submicroscopic NF1 contiguous gene deletions. Our refined map of the region will facilitate studies of the contribution of SLC6A4, CPD, and other contiguous genes to susceptibility to developmental/psychiatric disorders and to the phenotype(s) associated with NF1 contiguous gene deletions.

Keywords: serotonin transporter, CPD, NF1, YAC contig

INTRODUCTION

The endogenous indoleamine serotonin (5-hydroxytryptamine, 5-HT) functions as a neurotransmitter in the central and peripheral nervous systems. The actions of serotonin released into the synaptic cleft are terminated by reuptake into pre-synaptic nerve terminals via a high-affinity, Na⁺-dependent serotonin transporter (SERT) encoded by the SLC6A4 ('solute carrier family 6, member 4') gene. The SERT is the target for an important class of antidepressant drugs (the serotonin selective reuptake inhibitors) and also of certain drugs of abuse including 3,4-Methylenedioxymphetamine (MDMA or "ecstasy"). Polymorphic variation in the SLC6A4 gene has been reported by several laboratories to be associated with depression and other psychiatric disorders and to influence personality traits. For a review of the pharmacology and genetics of the SERT¹.

Detailed studies regarding the molecular basis of such associations would be facilitated greatly not only by knowledge of the SLC6A4 genomic structure and alternatively-spliced transcripts, but also by the chromosomal context in which the gene is located. For example, haplotype analyses and disequilibrium mapping of polymorphic sites both within and flanking SLC6A4 could provide strong evidence that the increased susceptibility is actually mediated by SERT and not the product of an unknown adjacent gene.

We report a precise map of a 1 Mb region encompassing the human SLC6A4 gene, which was previously mapped to chromosome 17 band q11.2-q12^{2,3}. Unexpectedly, the CPD gene, which encodes a metallopeptidase that is strongly implicated in protein processing during transit of the secretory pathway⁴, was also localised to the contig. Because the SLC6A4/CPD contig is centromeric to the NF1 gene, we evaluated whether these genes were commonly deleted in patients with neurofibromatosis type 1 (NF1) contiguous gene deletions.

MATERIALS AND METHODS

Construction and analyses of physical contig.

High density gridded filters of 4 human libraries, the RPC-1 PAC library⁵ and ICRF, and CEPH YAC libraries⁶⁻⁸ were screened using full length human SLC6A4 cDNA labelled with [α -³²P]dCTP (Ready-To-Go labelling beads, Pharmacia). Hybridisation was performed at 55°C for 20 hr in 0.5 M phosphate pH 7.2, 2.7% SDS, 1% BSA, and 1 mM EDTA. Filters were washed in 40 mM phosphate, 1 % SDS, 1 mM EDTA at 95°C and exposed to autoradiographic film (Fuji RX) at -70°C overnight. Positive clones were obtained from the UK MRC HGMP Resource Centre. For pulsed-field gel electrophoresis (PFGE), the yeast DNA was prepared by a modification of the methods of Schedl et al.⁹ and Bellis et al.¹⁰. YAC clones were inoculated into 15 ml of medium (Ura-/Trp-) with 2% of glucose as the carbon source. When cells had grown to late log phase after 2 - 4 days, low melting point (LMP) agarose plugs were made and subjected to Novozyme (Novo Biolabs) digestion for 4 - 6 hours. Plugs were washed in 50 mM EDTA (2 x 30 min) and digested with proteinase K (2 mg/ml) at 55°C overnight, in a buffer containing 0.5 M NaCl, 0.125 M Tris pH 8.0, 0.25 M Na₂EDTA, 1% (w/v) lithium sulphate, and 0.5 M β -mercaptoethanol. Plugs were washed with TE and stored at 4°C in 0.5 M EDTA.

Before use, agarose plugs were washed in TE (3 x 30 min), loaded onto 1% agarose gels and sealed with 1% LMP agarose in 0.5 x TBE buffer. Gels were run in 0.5 x TBE buffer at 6V/cm for 24 hours at 14°C with 60 seconds switch time and stained with ethidium bromide. DNA was fragmented by soaking gels in 0.25 M HCl for 15 min, denatured in 0.4 M NaOH for 3 x 20 min and blotted overnight onto Appligene Positive Membrane. Filters were neutralized with 25 mM phosphate pH 6.8/1 mM EDTA for 10 min and fixed for 2 min at full power (650W) in a microwave oven. Labeling of probes, hybridization and autoradiography were performed as above. Filters were stripped (3 x 15min in 0.1% SDS at 100°C) and exposed to autoradiography film overnight to ensure complete removal of probes between hybridizations. Four probes were used for construction of the contig: (i) a 854 bp Pst I fragment of SLC6A4 cDNA (corresponding to bp 785 - 1639, GenBank accession no. L05568), (ii) a 2.3 kb Eco RI - Pvu II fragment of pBR322 to detect the long YAC arm, (iii) 28L, a 3.2 kb Not I - EcoYRI fragment of PAC clone 50G6, which is ~40 kb 5' of the SLC6A4 gene, (iv) 24R, a 8.4 kb Not I - Hind III fragment of PAC clone 50G6, containing sequences ~15 kb 3' of the SLC6A4 coding sequence. For probes 28L and 24R, labeled DNA was pre-hybridized to human Cot-1 DNA (Gibco) for 15 min at 55°C before application to blots. YACs were sized by hybridization to pBR322 plasmid DNA, using the endogenous yeast chromosomes as size references.

The T_m for each primer oligonucleotide (Table 1) was calculated using the formula: $T_m = 69.3 + 41 \times \text{Ngc} / \text{Ntotal} - 650 / \text{Ntotal}$ (where Ngc is the number of G and C residues in a primer of total length Ntotal residues). The lower T_m value for each primer pair was used as the annealing temperature. Extension times were chosen according to the expected size of individual PCR products (approximately 1 min per 500 bp). PCR was performed for 30 or 35 cycles.

Patient and somatic cell hybrid lines

Patient UWA106-3 is hemizygous for a microdeletion of about 1-1.5 Mb that spans the entire NF1 gene¹²⁻¹³. The human/rodent somatic hybrid cell line UWA106-3-#36 harbors the patient's deleted chromosome 17, while the line UWA106-3-#41 harbors the non-deleted homolog 12. For fluorescence in situ hybridization (FISH), chromosome metaphase spreads from the lymphoblastoid cell line (UWA106-3) were prepared using standard methodology. DNA from PAC clone 50G6 was labeled with biotin-11-dATP by nick-translation (Gibco BRL). Hybridization was carried out as previously described by Edelhoff et al¹⁴ and signals were detected using a commercial system (Vector). The chromosomes were banded using Hoechst 33258-actinomycin D staining and counterstained with propidium-iodide. The chromosomes and signals were visualized by fluorescence microscopy using a dual band pass filter (Omega).

RESULTS

Characterization of the SLC6A4 gene and PAC clones

The size of the SLC6A4 gene was estimated by long-range PCR of human genomic DNA with 6 pairs of primers that cover the entire SLC6A4 gene from exon 1 to

14 (43084/43085, 43088/43089, 26373/2B, 54073/54074, 5A/5B, and 6A/P3, Table 1). PCR products of ~10, 3.5, 5, 4, 4 and >12 kb were obtained, respectively. We estimated that the SLC6A4 gene contained at least 15 exons and spans approximately 40 kb of genomic DNA.

To isolate genomic clones encoding the SLC6A4 gene, we screened the RPC-1 human PAC library by hybridization with full length human SLC6A4 cDNA. One of four positive PAC clones, designated 50G6, appeared to contain the entire coding sequence of the SLC6A4 gene and 5' and 3' untranslated regions as determined by PCR using primers described in Table 1. FISH with the 50G6 probe confirmed its location to proximal chromosome 17q as expected (data not shown) and indicated that the clone was not chimeric. Fragments from both ends of the insert in 50G6 were cloned into pBluescript SK- and characterized. End clone 24R contained a 8.4 kb Not I-Hind III fragment that included the SP6 promoter sequence of the PAC vector pCYPAC2N. End clone 28L contained a 3.2 kb Not I-EcoRI fragment including the T7 promoter sequence from the vector. Southern blot analyses of NotI digested 50G6 DNA revealed a 40 kb fragment that hybridized to end clone 28L, a 55 kb fragment that hybridized to end clone 24R, and a 16 kb fragment from the PAC vector (data not shown). These results indicated that the PAC clone 50G6 contains approximately 40 kb of 5' flanking sequence, the entire SLC6A4 gene (40 kb) and about 15 kb of 3' flanking sequence.

Construction of SLC6A4 contig

From a screen of gridded human YAC libraries with a full length human SLC6A4 cDNA, six clones were selected for further analyses. Clones 704F1, 782E2, 765D1 are from the CEPH library and 35D8, 132C6, 49A9 are from the ICRF library. Figure 2 gives the estimated length of each clone (Materials and Methods). PCR with SLC6A4 primers that amplify fragments across the length of the gene (Table 1) demonstrated that 5 of the 6 YACs harbored the entire SLC6A4 gene. The exception was clone 704F1, which lacked the 5' untranslated region and first exon (Figure 2). Each clone was found to carry the 10 repeat allele of SCL6A4 intron 2 polymorphism, while the SLC6A4 promoter polymorphism varied^{15,16}. The clones from the ICRF library carried the short SLC6A4 allele, while those from the CEPH library carried the long allele.

The contig depicted in Figure 2 was assembled by analysis of the 6 YACs and the 50G6 PAC clone for the presence of 15 regional loci, including the PAC end clones 24R and 28L. In addition to SLC6A4, 8 loci mapped within the contig. Together, these data oriented the 3' end of the SLC6A4 gene towards the chromosome 17 centromere. In addition, the absence of D17S1249 from clone 704F1 and its presence in clone 49A9, mapped this highly informative tetranucleotide repeat polymorphism to a location of <15 kb centromeric to the 3' end of the SLC6A4 gene. The following loci did not amplify from any of the clones in the SLC6A4 contig: D17S1543, TIGR-A004R11, TIGR-A007E42, D17S317, SHGC37126, SHGC36334, and D17S1824.

The carboxypeptidase D gene maps telomeric to SLC6A4

The D17S2004 locus corresponds to bp 1283-1564 of the EST clone U90914 (GenBank). The first 651 nucleotides of U90914 were identical to the 3'-untranslated region immediately preceding the polyadenylation signal of the human carboxypeptidase D

gene (CPD; GenBank U65090, ¹⁷). This suggests that the U90914 EST is an alternatively polyadenylated transcript of carboxypeptidase D that has an additional 1279 basepairs of sequence.

The sequences of D17S2004 and D17S2009 markers were also found in a 163 kb genomic sequence from human chromosome 17 (GenBank AC006050: sequence of human BAC clone hRPK.268_F_2, Whitehead Institute/MIT Center for Genome Research, Human Genome Sequencing Project) which encodes the entire CPD gene. By using both forward primers of D17S2009 and D17S2004, a 2.1 kb PCR product was obtained from either human genomic or YAC (35D8, 765D1 and 49A9) DNA. Direct sequencing of the 2.1 kb PCR product confirmed its identity to the corresponding sequence in AC006050. To confirm the presence of the CPD gene in our YAC/PAC contig, two pairs of primers (cpd6740F/cpd6858R, and cpd1065F/cpd1768R) were designed from the CPD cDNA sequence. Primers cpd6740F and cpd6858R are 1 kb downstream of D17S2004 within the 3'-UTR of the CPD gene and amplified the expected 118 bp product from human genomic DNA. Primers cpd1065F and cpd1768R amplified a 2.7 kb sequence approximately 44 kb 5' of D17S2009. Based on PCR results of three overlapping YAC clones 35D8, 765D1 and 49A9 (Figure 2), we concluded that the CPD gene lies telomeric to the SLC6A4 gene.

Hemizygotic deletion of the SLC6A4 and CPD genes in a NF1 patient

Because the NF1 gene maps distal to SLC6A4, and patients have been reported with NF1 microdeletions ^{12,13} we tested whether the NF1 gene mapped within the contig. NF1 exons 1, 27a and 49.2 were amplified using previously described primers ¹⁸. None of the clones, however, yielded products indicating that the contig does not contain the NF1 gene (data not shown). Among the NF1 microdeletion patients reported, one in particular was appeared to be for loci that presumably mapped nearer the centromere than SLC6A4 ¹². Metaphase chromosomes prepared from immortalized lymphoblasts of subject UWA106-3, were subjected to fluorescence in situ hybridization using the SLC6A4-containing PAC 50G6 as the probe. Only one hybridization signal was observed, confirming that the microdeletion included the SLC6A4 locus (Figure 3a).

DNA from rodent/human somatic hybrid cell lines carrying either the deleted (UWA106-3-#36: Figure 3b lane 3) or non-deleted (UWA106-3-#41: Figure 3b lane 4) chromosome 17 of the patient were analysed by PCR to determine the extent of the deletion. The CPD gene was deleted in the patient, along with D17S2120 (Figure 3b). The entire SLC6A4 gene, from the promoter region to exon 14 was deleted in cell line UWA106-3-#36. However, the centromeric markers D17S1294 and D17S1549 were detected in both the #36 and #46 cell lines. We conclude that the centromeric breakpoint of the deletion in this patient lies in a region of less than 15 kb between exon 14 of the SLC6A4 gene and D17S1294. Assay of somatic hybrid cell lines carrying the deleted chromosome 17 homolog of 17 additional NF1 microdeletion patients ^{12,13,13a} revealed that neither the SLC6A4 nor the CPD gene was deleted.

DISCUSSION

We report here the construction of a 1 Mb YAC/PAC contig encompassing the SLC6A4 and CPD genes and eight marker loci. We determined that SLC6A4 is <15 kb telomeric to D17S1294 and the 3' end of the gene is oriented towards the centromere. The order of STS markers (cen-D17S975-D17S1549-D17S1294-SLC6A4-CPD/D17S2004/D17S2009-D17S2120-ter) is in general agreement with the data in the Genetic Location Database¹⁹, the Genethon human linkage map²⁰, the GDB Human Genome Database²¹ and in the database published by the Center for Medical Genetics, Marshfield, WI²². The sizes of two CEPH YAC clones (782E2 600 kb and 765D1 1000 kb) differed from those (1160 and 1340 kb) given in the Whitehead Institute/MIT Center for Genome Research, Human Genetic Mapping Project, Data Release 12 (July 1997). These difference may reflect errors in the original size determinations of the YAC clones or result from rearrangement or truncation of YAC DNA.

In previous studies the SLC6A4 gene has been mapped by Ramamoorthy et al.²³ to chromosome 17q11.2 - 17q12 using FISH and somatic cell hybrids, and by Gelernter et al.³ to 17q12 (flanked by D17S58 and D17S73) using a RFLP in the 3'-UTR (for which 'SLC6A4' and 'HTT' are synonyms in the Genome Database). Our results are consistent with those of Esterling et al.²⁴, who found close linkage of HTT to D17S1294, but differ in the order of D17S1294 and D17S2120. Surprisingly, these authors assigned different map positions to two markers (HTT and SGHC-11022) which should be coincident: the sequence of SGHC-11022 is nested within that of HTT.

The appearance of the markers D17S2009 and D17S2004 in our YAC contig suggested that the CPD gene might be present in this region. This was confirmed by PCR with primers from other regions of the CPD gene. Our results are in agreement with those of Riley et al.²⁵, who recently localized the gene to 17p11.1-q11.1/11.2 by use of a regional mapping panel derived from somatic cell hybrids containing different portions of chromosome 17. Although no disorder has directly been linked with the CPD gene, it is possible that deficiency in this gene might affect the processing of secreted proteins. A mutation in the closely related carboxypeptidase E (CPE) gene in fat/fat mice has been reported to result in defective proinsulin processing leading to obesity and hyperglycaemia²⁶.

FISH and PCR analyses confirmed that both the SLC6A4 and CPD genes were part of the contiguous gene deletion in one out of seventeen NF1 patients microdeletion patients tested. Although these data suggest that majority of microdeletion patients will not be haploinsufficient for SERT and carboxypeptidase D, the patient sample was biased due to selection by certain phenotype findings. The phenotype of patient UWA106-3 is consistent with that of other NF1 contiguous gene deletion patients in that he had an early age of onset of dermal neurofibromas, certain facial anomalies^{12,13, 13a}. Unlike the majority of NF1 microdeletion patients, however, UWA106-3 is mentally retarded with a childhood intelligence quotient of 46¹². It has been reported that certain SLC6A4 alleles appear to be associated with susceptibility to affective disorder and other psychiatric diseases¹, however, the role of SERT protein levels in normal brain development is unknown. Although patient UWA106-3 is now a 27 year old mentally retarded male, he has had no findings suggestive of a psychiatric disorder. In addition, the SLC6A4 gene is transiently expressed in craniofacial epithelial structures during development, which suggests a role for serotonin in craniofacial morphogenesis²⁷⁻²⁹.

Exposure of mouse embryos in culture to inhibitors of the serotonin transporter caused craniofacial malformations consistent with a direct action at serotonin uptake sites³⁰. Although little is known about the function of carboxypeptidase D, its putative role in post-translational processing⁴ suggests that haploinsufficiency could contribute to multiple unrelated physical manifestations in different body systems. The identification and fine mapping of additional NF1 microdeletion cases is required to assess putative roles for SERT or carboxypeptidase D in the craniofacial and/or severe tumor phenotype of these patients.

The identification of eight marker loci flanking the SLC6A4 gene will facilitate future studies of the role of the SERT protein in susceptibility to developmental and psychiatric disorders. This contig will also provide a centromeric anchor for chromosomal walking towards the NF1 gene which may lead to the discovery of other genes contiguous to NF1. Functional analysis of these genes should play an role in understanding of neurofibromatosis as well as other developmental/psychiatric disorders.

FIGURE LEGENDS

Figure 1: Analysis of YAC clones by pulsed-field gel electrophoresis and Southern blotting. (a) Resolution of YAC DNA by ethidium bromide staining. The sizes of yeast chromosomes from *S. cerevisiae* are shown in kb at the left. Lanes 1 to 7 are DNA from 793F2, 765D1, 704F1, 782E2, 641D5, 35D8 and 132C6 respectively; The blot was sequentially hybridized with (b) a 2.3 kb EcoRI - PvuII fragment of pBR322 DNA; (c) a 854 bp PstI fragment of SLC6A4 cDNA; (d) the subclone 28L and (e) the subclone 24R. DNA from initial preparations of 765D1 appeared to contain a contaminant, 450kb in size, which did not hybridize to probes within or flanking the SLC6A4 gene. Yeast DNA containing the 1000kb YAC was isolated from a single colony and used for subsequent analysis.

Figure 2: Mapping of the SLC6A4 and CPD genes to 17q11 in a YAC/PAC contig. (a) Physical map (not to scale) of the region of chromosome 17 between the centromere and D17S54 (b) diagram illustrating the extent of the deletion (---) in the patient UWA106-3. The centromeric breakpoint (arrow head) of the deletion lies between D17S1294 and the last exon of the SLC6A4 gene, (c) the positions of the SLC6A4 (□) and CPD (□) genes, STS markers and other probes in the 6 YAC clones and one PAC clone (50G6) used in construction of the contig. Sizes of the clones are indicated in brackets. Probable regions of chimerism in YACs 704F1 and 132C6 are shaded. The orientations of the YAC vector arms for clones 35D8 and 132C6 are indicated with L (for long arm) and S (for short arm). Orientation of the genomic insert in the PAC clone 50G6 is shown relative to the SP6 and T7 promoters of the PAC vector. The 3' end of the SLC6A4 gene is oriented towards the centromere. Circles represent the presence of STS markers and probes (28L and 24R), detected by PCR and by Southern hybridization in YAC/PAC clones and in the UWA106-3-#36 hybrid line carrying the deleted chromosome 17 of the patient.

Figure 3: (a) The SLC6A4 gene is deleted in an NF1 microdeletion patient. Metaphase chromosome preparations from lymphoblasts of patient UWA106-3 were hybridized with 50G6 PAC DNA. The two chromosomes 17 are indicated by an arrow: only one of them hybridized to the SLC6A4 probe, (b) Localization by PCR of the centromeric breakpoint of the deletion in patient UWA106-3. DNA templates were as follows: (lane 1) YAC 765D1; (lane 2) genomic DNA from patient UWA106-3; (lane 3) cell line UWA106-3-#36 carrying the deleted chromosome 17; (lane 4) cell line UWA106-3-#41 carrying the non-deleted chromosome 17; (lane 5) the Chinese hamster RJK cell line from which somatic cell hybrid lines UWA106-3-#36 and UWA106-3-#41 were derived. The primers (see Table 1 and the Genome Database [<http://gdbwww.gdb.org>]) and the size of the PCR products are indicated at the right. The specific PCR product of the E2F/2B primer pair is arrowed. Note that the centromeric breakpoint of the deletion lies between D17S1294 and exon 14 (defined by primer P3) of the SLC6A4 gene.

REFERENCES

- 1 Lesch KP. Molecular biology, pharmacology and genetics of the serotonin transporter: psychobiological and clinical implications. In: Baumgarten HG, G-thert M, editors. Serotonergic neurons and 5-HT receptors in the CNS. Volume 129, Handbook of Experimental Pharmacology. Berlin and Heidelberg: Springer-Verlag; 1997. p 671-705.
- 2 Bradley CC, Blakely RD. Alternative splicing of the human serotonin transporter gene. *J. Neurochem.* 1997;69: 1356-67.
- 3 Gelernter J, Pakstis AJ, Kidd KK. Linkage mapping of serotonin transporter protein gene SLC6A4 on chromosome 17. *Hum. Genet.* 1995;95: 677-80.
- 4 Varlamov O, Fricker LD. Intracellular trafficking of metallopeptidase D in AtT-20 cells: localization to the trans-Golgi network and recycling from the cell surface. *J. Cell Sci.* 1998;111: 877-85.
- 5 Ioannou PA, Amemiya CT, Garnes J et al. A new bacteriophage P1-derived vector for the propagation of large human DNA fragments. *Nat. Genet.* 1994;6: 84-9.
- 6 Anand R, Riley JH, Butler R, Smith JC, Markham AF. A 3.5 genome equivalent multi access YAC library: construction, characterisation, screening and storage. *Nucleic Acids Res.* 1990;18: 1951-6.
- 7 Larin Z, Monaco AP, Lehrach H. Yeast artificial chromosome libraries containing large inserts from mouse and human DNA. *Proc Natl Acad Sci U S A* 1991;88: 4123-7.
- 8 Chumakov IM, Le Gall I, Billault A et al. Isolation of chromosome 21-specific yeast artificial chromosomes from a total human genome library. *Nat. Genet.* 1992;1: 222-5.
- 9 Schedl A, Montoliu L, Kelsey G, Schutz G. A Yeast Artificial Chromosome Covering the Tyrosinase Gene Confers Copy Number-Dependent Expression In Transgenic Mice. *Nature* 1993;362: 258-261.
- 10 Bellis M, Pages M, Roizes G. A simple and rapid method for preparing yeast chromosomes for pulsed field gel electrophoresis. *Nucleic Acids Res.* 1987;15: 6749.
- 12 Kayes LM, Burke W, Riccardi VM et al. Deletions spanning the neurofibromatosis 1 gene: identification and phenotype of five patients. *Am. J. Hum. Genet.* 1994;54: 424-36.
- 13 Leppig KA, Viskochil D, Neil S et al. The detection of contiguous gene deletions at the neurofibromatosis 1 locus with fluorescence in situ hybridization. *Cytogenet. Cell Genet.* 1996;72: 95-8.
- 13a. Leppig K, Kaplan P, Viskochil D, Weaver M, Orterberg J, Stephens K (1997) Familial neurofibromatosis 1 gene deletions: cosegregation with distinctive facial features and early onset of cutaneous neurofibromas. *Am J Med Genet* 73:197-204
- 14 Edelhoff S, Ayer DE, Zervos AS et al. Mapping of two genes encoding members of a distinct subfamily of MAX interacting proteins: MAD to human chromosome 2 and mouse chromosome 6, and MXI1 to human chromosome 10 and mouse chromosome 19. *Oncogene* 1994;9: 665-8.
- 15 Heils A, Teufel A, Petri S et al. Allelic variation of human serotonin transporter gene expression. *J. Neurochem.* 1996;66: 2621-2624.

- 16 Ogilvie AD, Battersby S, Bubb VJ et al. A polymorphism of the serotonin transporter gene is associated with susceptibility to major affective disorder. *Lancet* 1996;347: 731-733.
- 17 Tan FL, Rehli M, Krause SW, Skidgel RA. Sequence of human carboxypeptidase D reveals it to be a member of the regulatory carboxypeptidase family with three tandem active site domains. *Biochem. J.* 1997;327: 81-87.
- 18 Li Y, O'Connell P, Breidenbach HH et al. Genomic organization of the neurofibromatosis 1 gene (NF1). *Genomics* 1995;25: 9-18.
- 19 Collins A, Teague J, Keats BJ, Morton NE. Linkage map integration. *Genomics* 1996;36: 157-62.
- 20 Dib C, Faure S, Fizames C et al. A comprehensive genetic map of the human genome based on 5,264 microsatellites. *Nature* 1996;380: 152-4.
- 21 Fasman KH, Letovsky SI, Li P, Cottingham RW, Kingsbury DT. The GDB Human Genome Database Anno 1997. *Nucleic Acids Res.* 1997;25: 72-81.
- 22 Broman KW, Murray JC, Sheffield VC, White RL, Weber JL. Comprehensive Human Genetic Maps: Individual and Sex-Specific Variation in Recombination. *Am. J. Hum. Genet.* 1998;63: 861-9.
- 23 Ramamoorthy S, Bauman AL, Moore KR et al. Antidepressant- and cocaine-sensitive human serotonin transporter: molecular cloning, expression, and chromosomal localization. *Proc Natl Acad Sci U S A* 1993;90: 2542-6.
- 24 Esterling LE, Yoshikawa T, Turner G et al. Serotonin transporter (5-HTT) gene and bipolar affective disorder. *Am. J. Med. Genet.* 1998;81: 37-40.
- 25 Riley DA, Tan F, Miletich DJ, Skidgel RA. Chromosomal localization of the genes for human carboxypeptidase D (CPD) and the active 50-kilodalton subunit of human carboxypeptidase N (CPN1). *Genomics* 1998;50: 105-8.
- 26 Naggert JK, Fricker LD, Varlamov O et al. Hyperproinsulinaemia in obese fat/fat mice associated with a carboxypeptidase E mutation which reduces enzyme activity. *Nat. Genet.* 1995;10: 135-42.
- 27 Lauder JM, Zimmerman EF. Sites of serotonin uptake in epithelia of the developing mouse palate, oral cavity, and face: possible role in morphogenesis. *J. Craniofac. Genet. Dev. Biol.* 1988;8: 265-76.
- 28 Lauder JM, Tamir H, Sadler TW. Serotonin and morphogenesis. I. Sites of serotonin uptake and -binding protein immunoreactivity in the midgestation mouse embryo. *Development* 1988;102: 709-20.
- 29 Shuey DL, Sadler TW, Tamir H, Lauder JM. Serotonin and morphogenesis. Transient expression of serotonin uptake and binding protein during craniofacial morphogenesis in the mouse. *Anat Embryol (Berl)* 1993;187: 75-85.
- 30 Shuey DL, Sadler TW, Lauder JM. Serotonin as a regulator of craniofacial morphogenesis: site specific malformations following exposure to serotonin uptake inhibitors. *Teratology* 1992;46: 367-78.
- 31 Cnossen MH, van der Est MN, Breuning MH et al. Deletions spanning the neurofibromatosis type 1 gene: implications for genotype-phenotype correlations in neurofibromatosis type 1? *Hum. Mutat.* 1997;9: 458-64.

Table 1. PCR Primers for SLC6A4 and CPD genes

Forward Primers (5' - 3')	Reverse Primers (5' - 3')	Product	Size
31013 CACCTAACCCCTAATGTCCCTACT	31014 GGAAGTGGCTGGACAACCCAC	SLC6A4 5-HTTLPR	458/502 bp
1AP(F) GCGTCTAGGTGGCACCAGAATC	1AP(R) TCGCGCTTGTGTTCCAGCTAC	SLC6A4 Exon 1a	545 bp
43084 CCTGCGAGGAGGCGAGGAGG	43085 AACTCCTCTCGGTGACTAATCG	SLC6A4 Exon 1-Intron 1a	10 kb
44771 CTAGTGACTGACATTCCTGG	44772 TGTCCAGTCTATCTGCACATG	SLC6A4 Exon 1b	824 bp
43088 GCCTGGCGTTGCCGCTCTGAATGC	43089 TAGCAGCAGCAGTGAGCAGTTACC	SLC6A4 Intron 1a-Exon 2	3.5 kb
26373 ACTAACCCAGCAGGATGGAGACG	26374 TAGAGTCCCGTGTGTCATCTCC	SLC6A4 Exon 2	199 bp
18564 GTCAGTATCACAGGCTGCGAG	18565 TGTTCCTAGTCTTACGCCAGTG	SLC6A4 Intron 2 VNTR	249/266/299 bp
26373 ACTAACCCAGCAGGATGGAGACG	2B TTAGACCCGGTGGATCTGCAG	SLC6A4 Exons 2-5	5 kb
54073 TGGCAAGGTGAGGAAGGCTCTGG	54074 CCACCTCAGACACATCTTCATTCC	SLC6A4 Exons 5-8	4 kb
5A ATGAAGATGTGTCTGAGGTGG	5B ACAGCGACTGCTTCGATCAG	SLC6A4 Exons 8-11	3.8 kb
6A TACGTGGTGAAGCTGCTGGA	P3 GAGGAGGAGGTGTGGAGAAGCC	SLC6A4 Exons 11-14	>12 kb
26375 AGTTCTGATGAGGCACGC	26376 TTCATCACCTCCATCCACATCC	SLC6A4 Exon 14	223 bp
60703 ATCACATTAGAACTGTCTTGTTCG	60704 AGGTATCTATGAGGTTCAACAGC	CPD 1065F + CPD 1768R	2.7 kb
60705 TTATGTAGTTTCAAGTAAGATGTGCC	60706 GCAAGTATTTCTCAACTGGATAGG	CPD 6740F + CPD 6858R	118 bp

Table 2. Characterization of YAC/PAC clones containing the SLC6A4 and CPD genes

Mb	Locus	704F1 640 kb	50G6 95 kb	782E2 600 kb	132C6 630 kb	35D8 500 kb	765D1 1000 kb	49A9 230 kb	793F2 1600 kb	641D5 140 kb	16FC9 820 kb
28.040	D17S1543	-	-	-	-	-	-	-	-	-	-
	TIGR-A004R11	-	-	-	-	-	-	-	-	-	-
	TIGR-A007E42	-	-	-	-	-	-	-	-	-	-
28.061	D17S1317	-	-	-	-	-	-	-	-	-	-
	SHGC37126	-	-	-	-	-	-	-	-	-	-
	SHGC36334	-	-	-	-	-	-	-	-	-	-
28.191	D17S1824	-	-	-	-	-	-	-	-	-	-
28.253	D17S975	-	-	-	-	-	-	-	-	-	-
28.373	D17S1549	+	-	+	-	+	+	-	-	-	-
	24R (probe)	+	+	+	+	+	+	NE	-	-	NE
28.318	D17S1294	+	+	+	+	+	+	-	-	-	-
	SLC6A4 exon 14	+	+	+	+	+	+	+	+	+	-
	SLC6A4 exon 5-8	+	+	+	+	+	+	+	+	+	-
	SLC6A4 exon 2-5	+	+	+	+	+	+	+	+	+	+
	SLC6A4 intron 2 VNTR	10	10	10	10	10	10	10	10	-	10
	SLC6A4 exon 2	+	+	+	+	+	+	+	+	-	+
	SLC6A4 exon 1B	+	+	+	+	+	+	+	+	-	+
	SLC6A4 1AP	-	+	+	+	+	+	+	+	-	+
	SLC6A4 5'HTTLPR	-	+	L	S	S	L	+	L	-	NE
	28L (probe)	-	+	+	+	+	+	NE	+	-	NE
	CPD6740/6858	-	-	-	-	+	+	+	-	-	-
28.454	D17S2009	-	-	-	-	+	+	+	-	-	-
28.521	D17S2004	-	-	-	-	+	+	+	-	-	-
	CPD1065/1768	-	-	-	-	+	+	+	-	-	-
	D17S2120	-	-	-	-	-	+	+	-	-	-
	NF1 exon 1	-	-	-	-	-	-	-	-	-	-
	WI-9201	-	-	-	+	-	-	-	-	-	-
	NF1 exon 27a	-	-	-	-	-	-	-	-	-	-
	NF1 exon 49.2	-	-	-	-	-	-	-	-	-	-
	Chimerism	CS	NCF	NE	NCF	NCF	NE	CF	CS	CS	CS

Caption for Table 2

YAC/PAC DNA were analysed by PFGE, hybridisation, FISH, and PCR for STS markers and other primers. NCF: not chimeric demonstrated by FISH; CF: chimeric revealed by FISH; CS: Chimeric determined by Southern hybridization and STS analyses; NE: not examined.(+): positive by PCR or hybridization, (-): negative by PCR or hybridization. Alleles of the polymorphism in the SLC6A4 promoter region (5'HTTLPR) are indicated by L (long form) and S (short form), and the VNTR in intron 2 was the 10 repeat allele (10) for all YACs tested. Loci 28L and 24R are from hybridisation data. YAC sizes were determined by hybridisation with pBR322 plasmid DNA. Distances (in Mb) from 17pter to markers are from the Genetic Location Database (Collins et al.,1996b).Primers for the NF1 gene are based on Li et al. (1995) and for STS markers on the Genome Database [<http://gdbwww.gdb.org>].

FIGURE 1

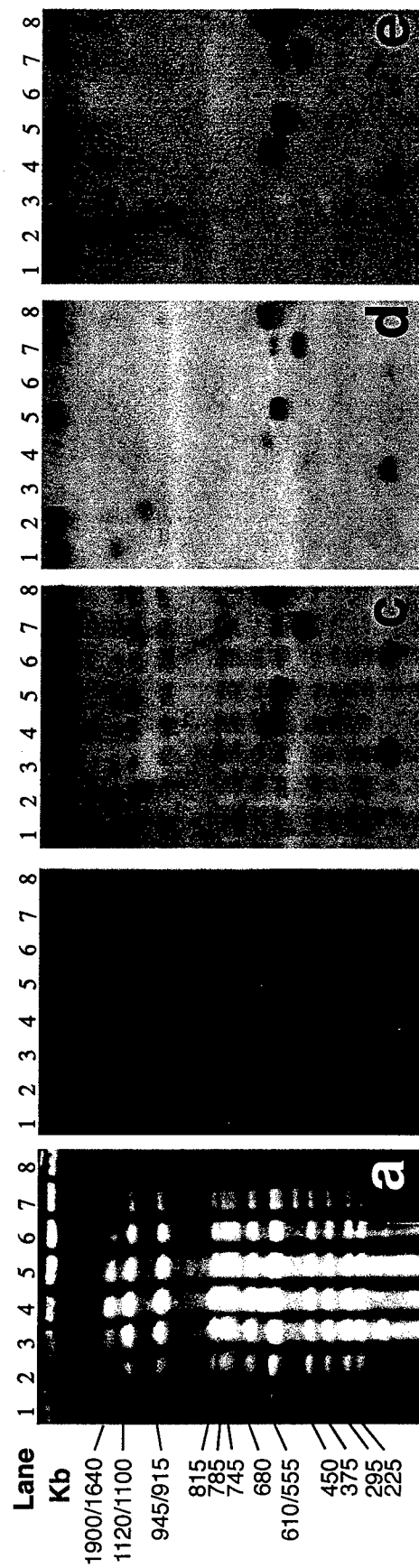


FIGURE 2

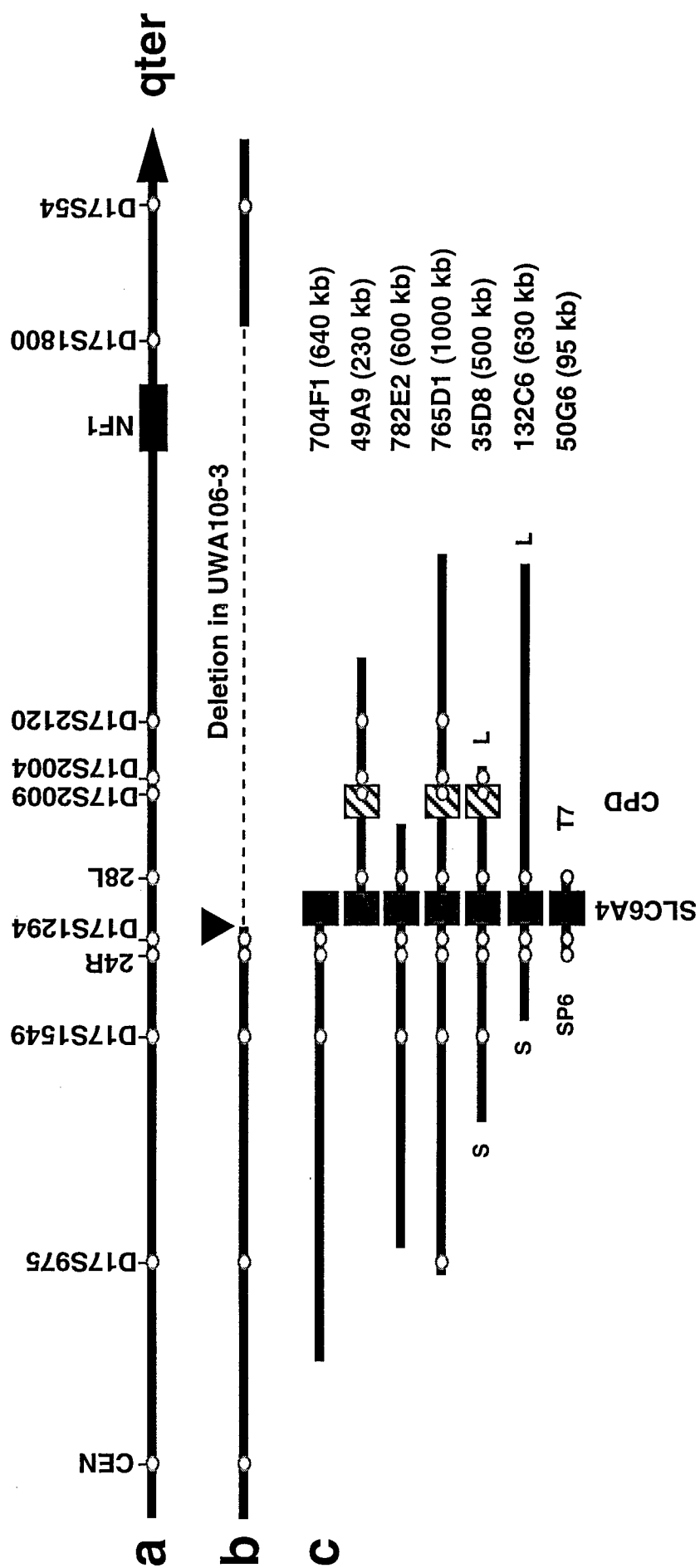


FIGURE 3A

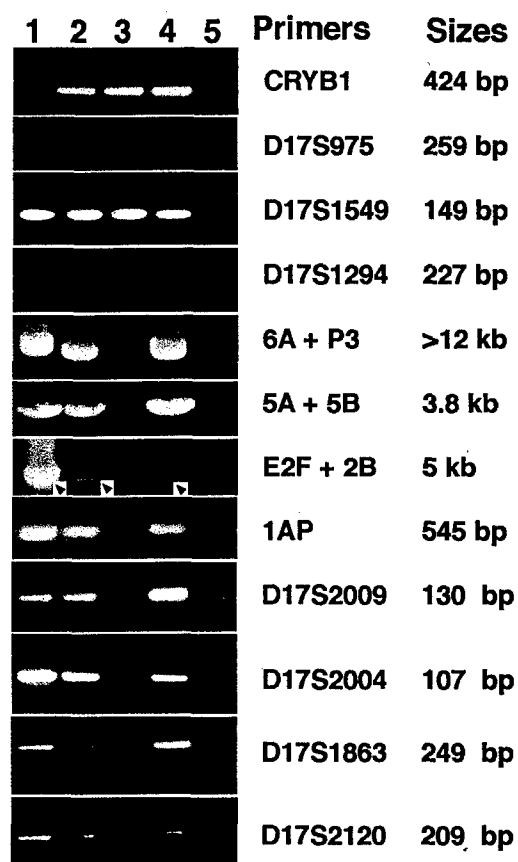
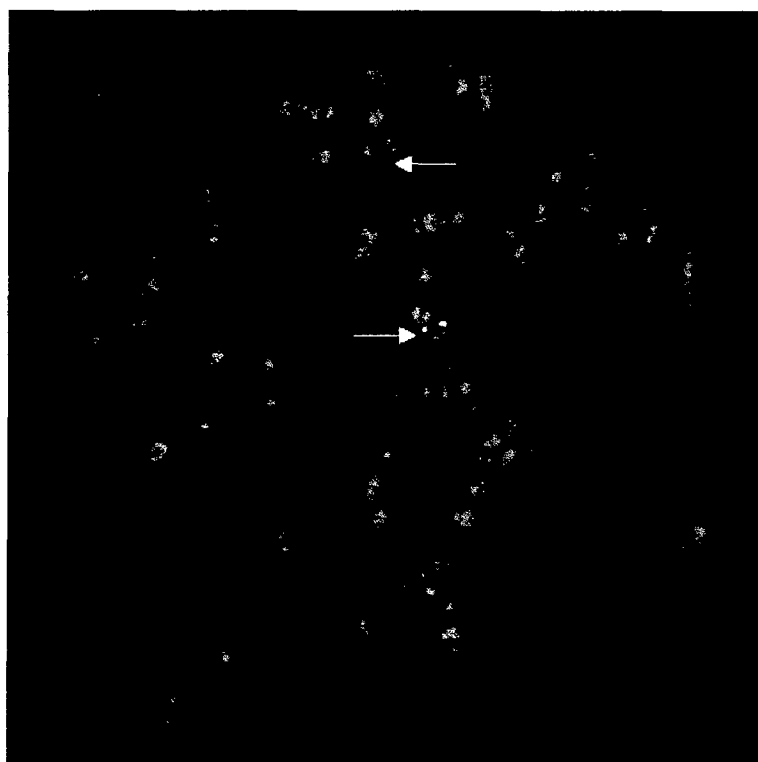


FIGURE 3B



NF1 microdeletion breakpoints are clustered at flanking repetitive sequences

Michael O. Dorschner, Department of Medicine, University of Washington, Seattle, WA 98195 USA

Virginia P. Sybert, Department of Medicine, University of Washington, Seattle, WA 98195 USA

Molly Weaver, Department of Medicine, University of Washington, Seattle, WA 98195 USA

Beth A. Pletcher, Department of Pediatrics, University of Medicine and Dentistry- New Jersey Medical School,
Newark, NJ 07103 USA

Karen Stephens, Departments of Medicine and Laboratory Medicine, University of Washington, Seattle, WA 98195 USA

Corresponding author:

Michael O. Dorschner, PhD

University of Washington,

1959 NE Pacific St. Room I-204, Medical Genetics Box 357720, Seattle, WA 98195

206-685-9066, FAX 685-4829, mod@u.washington.edu

Genbank accession numbers: AF170177-AF170186.

ABSTRACT

Neurofibromatosis type 1 patients with a submicroscopic deletion spanning the *NF1* tumor suppressor gene are remarkable for an early age at onset of cutaneous neurofibromas, suggesting the deletion of an additional locus that potentiates neurofibromagenesis. Construction of a 3.5 Mb BAC/PAC/YAC contig at chromosome 17q11.2 and analysis of somatic cell hybrids from microdeletion patients showed that 14 of 17 cases had deletions of 1.5 Mb in length. The deletions encompassed the entire 350 kb *NF1* gene, 3 additional genes, 1 pseudogene and 16 ESTs. In these cases, both proximal and distal breakpoints mapped at chromosomal regions of high identity, termed NF1REPs. These REPs, or clusters of paralogous loci, are 15-100 kb and harbor at least 4 ESTs and an expressed SH3GL pseudogene. The remaining 3 patients had at least one breakpoint outside of an NF1REP element; one had a smaller deletion thereby narrowing the critical region harboring the putative locus that exacerbates neurofibroma development to 1 Mb. These data show that the likely mechanism of *NF1* microdeletion is homologous recombination between NF1REPs on sister chromatids. NF1 microdeletion is the first REP-mediated rearrangement identified that results in loss of a tumor suppressor gene. Therefore, in addition to the germline rearrangements reported here, NF1REP-mediated somatic recombination could be an important mechanism for the loss of heterozygosity (LOH) at *NF1* in tumors of NF1 patients.

INTRODUCTION

Haploinsufficiency for neurofibromin is the molecular basis of neurofibromatosis type 1 (NF1), a common autosomal disorder that predisposes to the development of benign and malignant tumors. Genetic, biochemical, and proliferative studies of cells from NF1-associated tumors are consistent with a tumor suppressor function for neurofibromin. Tumor suppressor activity is due, at least in part, to a ras-GAP (GTP-ase activating protein) domain which accelerates the conversion of activated GTP-ras to inactivated GDP-ras (1). Evidence in human and mouse show that neurofibromin-deficient tumor cells have increased activated ras and dysregulated proliferative properties (2,3), which may be mediated by the ras-dependent mitogen-activated protein kinase signaling pathway (4). Both benign and malignant tumors show homozygous inactivation of *NF1* resulting in lack of functional neurofibromin. Although *NF1* inactivation in a tumor progenitor cell can occur by numerous mechanisms, the identification of defined intragenic *NF1* mutations in primary tumor tissue argues that lack of neurofibromin is central to their development (5-7).

Over 70% of germline mutations of the *NF1* gene are intragenic and predict a premature truncation of neurofibromin (8). These mutations are distributed throughout the coding region. They are generally unique for a given patient or family, and are not predictive for any of the diverse clinical manifestations that can develop in this multisystemic disorder. Nearly all NF1 patients develop café-au-lait macules, axillary and inguinal freckling, multiple neurofibromas, and Lisch nodules, which are hamartomas of the iris of the eye. Other significant, but less common, manifestations of the disorder include learning disabilities, optic glioma, bony abnormalities (sphenoid bone dysplasia, pseudoarthrosis, scoliosis), increased risk of specific malignancies, and others (9,10). NF1 has been considered to be primarily a disorder of cells derived from the neural crest, which is supported by recent evidence consistent with neurofibromas arising by clonal proliferation of a neurofibromin-deficient Schwann cell (11).

Previously, we identified 5 patients that carried a deletion of one entire *NF1* allele. These patients were remarkable for an early age (<10 years) at onset of dermal neurofibromas, an increased number or heavy burden of neurofibromas relative to their age, and certain atypical facial features (12,13). The association of an *NF1* microdeletion with this phenotype was subsequently confirmed by us and other investigators (14-18). In addition, the identification of families segregating an *NF1* microdeletion demonstrated that the rearrangement was co-inherited with the remarkable facial and tumor features (17,19,20).

The molecular basis for precocious neurofibromagenesis in microdeletion patients is unknown. Previously, we estimated the microdeletions at 0.7 - 2 Mb, which, even accounting for the large 350 kb *NF1* gene, implies that many additional genes are also deleted (13,14,19). Theoretically, early age at onset of neurofibromagenesis could be attributed to (1) deletion of the *NF1* gene alone, (2) co-deletion of *NF1* and one of the three genes of unknown function that are embedded in an *NF1* intron, (3) co-deletion of *NF1* and a novel contiguous gene(s), or (4) dysregulation of a gene at the deletion breakpoint. We consider it unlikely that neurofibromin haploinsufficiency alone could account for early onset of tumorigenesis. Over 70% of NF1 patients are heterozygous for a mutation that predicts premature truncation of

neurofibromin, yet in a population-based study only about 14% of subjects developed dermal neurofibromas before 10 years of age (21,22). However, it is unknown whether neurofibroma development could be ameliorated in any of these patients due to possible residual activity from the mutant *NF1* allele. The role of a putative co-deleted locus has been difficult to assess because the number of deletion patients is small and information regarding number and age at onset of neurofibromas and deletion magnitude are not always evaluated or reported. Recently, however, we described 12 unrelated *NF1* microdeletion patients with early onset and/or high burden of neurofibromas with deletion breakpoints that clustered in the same centromeric and telomeric locus intervals (K. Maruyama et al, submitted). Towards mapping and identifying a locus that potentiates neurofibromagenesis in *NF1* patients, we constructed a 3.5 Mb physical map of the *NF1* region, precisely mapped the deletion, and examined deletion genotype with patient phenotype. We report that the breakpoints in the majority of patients are clustered at flanking genomic segments of paralogous sequence (sequence similarity due to duplication). These results have important implications regarding germline and somatic rearrangements involving *NF1*.

RESULTS

Construction of a 3.5 Mb contig

Recently, we determined that both the centromeric and telomeric breakpoints in 14 out of 15 *NF1* patients with submicroscopic deletions were clustered in two distinct marker intervals. Quantitative PCR and the analysis of somatic cell hybrid lines carrying deleted chromosome 17 of each patient mapped the centromeric breakpoints between marker loci *D17S2120* and *UT172* and the telomeric breakpoints between *D17S1800* and *D17S1880* (K. Maruyama et al., submitted; Figure 1). Although these data were suggestive of breakpoint clustering, the length of each interval was unknown. In addition, the number and unique order of other markers within each of these initial breakpoint intervals was unknown. To refine the location of the deletion breakpoints, we sought to construct a physical map encompassing both breakpoint cluster regions. Initially, chromosome 17 loci reported to map at or near band q11.2 were gleaned from the literature and publicly-available electronic databases and screened by PCR against a somatic cell hybrid mapping panel. This placed each locus into one of five possible chromosomal intervals (Figure 1). Loci that mapped to intervals C and D were used to identify and construct a contig of novel and previously reported BAC and PAC clones. Initial database searches identified 5 sequenced clones that served as a framework for contig construction. Two BACs, 468F23 and 41C23, were found to harbor *AH1* and *AN2* respectively, which are end sequences of a previously described *NF1* YAC contig (23)(Figure 2). A 297 kb sequence carrying a large portion of the *NF1* gene (Genbank #AC004526), and clones 542B22 and 307A16, were identified from database searches. Together, the 3 clones 499I20, AC004526, and 41C23 comprise a 476 kb contiguous sequence spanning from intron 1 of the *NF1* gene to *D17S1800* (Figure 2). The remainder of the contig was assembled by screening a BAC library with selected loci that mapped in intervals C and D (Figures 1,2) and by utilizing newly released chromosome 17 sequences from the Whitehead Institute for Biomedical Research/MIT Center for Genome Research (<http://www-genome.wi.mit.edu/>). The clones comprising the BACs are listed in Table 1.

The contig consisted of 39 BAC/PAC and 2 YAC clones (Figure 2, Table 1). The new marker *A16INT* linked together the 2 YACs y947g11 and y815b11 (<http://www-genome.wi.mit.edu/>), creating a YAC contig of the region. In addition, loci prominent for their previous use in genetic mapping and loss of constitutional heterozygosity (LOH) analyses were mapped precisely. *UT172*, previously estimated to be 1.5 Mb centromeric of *NF1* (24), is only ~250 kb distant within BAC 468F23. *D17S117* and *D17S120* are located approximately 1 Mb centromeric of *NF1*; the latter marker actually lies within an intron of the carboxypeptidase D (*CPD*) gene. *D17S798* is located about 1.8 Mb telomeric of *NF1*.

Fine mapping of the *NF1* microdeletion breakpoints

Over 10 loci were placed precisely in each of the breakpoint cluster regions (Figure 1), thereby facilitating fine mapping of the breakpoints of all 17 microdeletion patients. Fourteen microdeletion patients had proximal breakpoints in the locus interval of *SH3GLP2* to *CYTOR4* (*SHGC-37343*) and distal breakpoints in the interval between *SH3GLP1* and *D17S1880* (Figure 2). The remaining 3 deletion cases had at least one novel breakpoint (Figure 2). Patient UWA113-1 had a novel centromeric breakpoint between *FB12A2* and exon 1 of the *NF1* gene. Both breakpoints of patient UWA155-1 were novel and located between the intervals defined by *SHGC35088* - *FB12A2* and *D17S1656* - *stSG50857*. Patient UWA106-3, who has the largest deletion in our cohort (13) also had two unique breakpoints. The telomeric breakpoint mapped in the

interval of *D17S73* to *FB6F10* and the centromeric breakpoint was mapped previously between *D17S1294* and *SCL6A4* during construction of a physical contig of the latter gene that encodes the serotonin transporter (25).

The contig provided more precise estimates of the physical lengths of both the region and the patient deletions. Because YACs 947g11 and 815b11, each estimated at 1.7 Mb (<http://www-genome.wi.mit.edu/>), are completely contained within the deletion of UWA106-3, this patient's deletion is approximated at 3.5 Mb. YAC 947g11 spans from *SLC6A4* to *A16INT* and overlaps 815b11, which extends to just beyond *D17S798*. The known lengths of sequenced BAC and the average length of 185 kb for nonsequenced BACs derived from the RPC1-11 library, were subtracted from the YAC lengths to give the estimated scale in Figure 2. The length of the common *NFI* microdeletion was estimated at 1.5 Mb.

***NFI* microdeletion breakpoints cluster at repetitive sequences**

Fine mapping of the region led to the discovery of two *SH3GL* expressed pseudogenes, *SH3GLP2* and *SH3GLP1*, that mapped near the breakpoints of the common *NFI* deletions (Figure 2). Because low copy repeats are known to flank deletions/duplications responsible for some contiguous gene syndromes (26), a search for additional multicopy transcripts was initiated. A third expressed pseudogene, *SH3GLP3*, was reported to map distally at 17q24 (27). BLAST analyses of the *SH3GL* pseudogenes identified BACs 271K11 and 147L13, which carried *SH3GLP2* and *SH3GLP3*, respectively. The STS/EST content of the BAC clones was obtained (<http://www-genome.wi.mit.edu/>) and BLAST analyses identified their locations within each clone. This revealed that two ESTs, *WI-12393* and *WI-9461*, were present in both BACs and located near each respective *SH3GL* pseudogene. Systematic BLAST analyses of loci reportedly mapping near *NFI* in publicly-available genome databases revealed that *stSG40093* and *stSG31654* were not only in BAC 271K11 centromeric to *NFI*, but were also harbored by BAC 147L13 at chromosome 17q24 (<http://www.ncbi.nlm.nih.gov/genemap98>). Together these analyses identified two clusters of five transcripts for which the order and relative distance between markers was conserved. These clusters of paralogous loci were designated as NFIREP using the suffixes -P and -D to distinguish the proximal repeat at 17q11.2 from the distal repeat at 17q24 (Figures 2, 3).

To determine if the unsequenced region surrounding *SH3GLP1* comprised an additional NFIREP, PCR primers for *WI-9461*, *stSG31654*, *stSG40093*, and *WI-12393* were used to amplify these loci from BACs overlapping the *SH3GLP1* locus. BAC clones 953C18, 951F11, and 95306 were positive for each of the transcripts; 999E22 was positive for all but the *WI-12393* locus. This medially positioned repeat cluster was designated NFIREP-M (Figure 3). These results demonstrated that chromosome 17 carries at least 3 clusters of paralogous loci: *WI-9461*, *stSG31654*, *stSG40093*, and *WI-12393*, each in association with a specific *SH3GL* pseudogene (Figure 3). The absence of *WI-12393* from BAC 999E22 and preliminary sequence analysis (M. Dorschner, unpublished data) strongly suggests that NFIREP-P and -M are direct repeats of 15-100 kb in length. The repetitive sequences may extend farther beyond *WI-12393*. The breakpoints of the patients carrying the common *NFI* microdeletion lie within, or adjacent to, NFIREP regions. The centromeric breakpoints were between *SH3GLP2* and *CYTOR4*, while the telomeric breakpoints occurred between *SH3GLP1* and *K8CEN*. Finer mapping of the breakpoints will require the development of REP-specific primers or Southern blot analyses that identify junction fragments. The size and orientation of NFIREP-D is unknown.

Several lines of evidence confirmed that, despite carrying sequences with a high degree of identity, BACs spanning NFIREP-P and NFIREP-M were localized unambiguously. First, the primers for amplification of *SH3GLP1* and *SH3GLP2* were locus-specific, exploiting base differences in the 5' region of the transcripts (27). BACs 943L10 and 946G8 were the only clones that possessed *SH3GLP2*, while clones 953C18, 951F11, 999E22, and 95306 carried only *SH3GLP1*. In addition, these BACs harbored the expected unique loci based on our deletion analysis. BAC 943L10 was positive for *D17S1863* and *CYTOR4*, while BACs spanning the medial REP contained *KIAA0160* or *D17S1880*.

Mouse orthologs for all of the genes located in interval B (Figure 1), *SLC6A4*, *CPD*, *CDK5R1* and the chemokine cluster, have been mapped to the same region of mouse chromosome 11 that carries the *NFI* ortholog. It appears that synteny has been conserved between human and mouse for the region from *CRYBA1* to at least the chemokine cluster.

***NFI* deletion genotype/phenotype and parental origin of deletion**

The physical features of the 13 unrelated *NFI* microdeletion patients and the 4 members of family UWA166 are summarized in Table 4. There were no obvious differences detected between the features present in those individuals with the common *NFI* deletion and the three with deletions of different lengths. No single feature was present or absent

consistently within either group. The location of the putative gene that potentiates neurofibromagenesis was narrowed to an interval of 1 Mb between *FB12A2* and *SH3GLP1*, as defined by the deletion of patient UWA113-1 (Figure 2). This critical region is known to harbor 4 genes, 2 pseudogenes, and 7 ESTs (Figure 2, Table 3).

A preference for *de novo* microdeletion of the maternally derived chromosome was observed. Among the 8 cases with documented *de novo* microdeletions, 6 were derived from the maternal homolog (UWA patients 113-1, 119-1, 147-3, 167-1, 183-1, 184-1) and 2 from the paternal homolog (UWA106-3, UWA123-3) (13,19, data not shown). Three families inherited NF1 microdeletions. Family UWA166 includes the affected mother UWA166-1 and her 3 affected children UWA166-2, -3, -4 (19), patient UWA169-1 inherited NF1 from his affected mother (19,28), and UWA155-1 inherited NF1 from his affected father.

DISCUSSION

NF1REP elements

Three NF1REPs were mapped to chromosome 17. NF1REP-P and -M flank the *NF1* locus at 17q11.2 and are separated by ~1.5 Mb of DNA. The third, NF1REP-D, is located at 17q24. Each REP is composed of at least five transcripts/ESTs including a *SH3GL* pseudogene, *WI-9461*, *stSG31654*, *stSG40093*, and *WI-12393* (Figure 3). In a search for proteins containing SH3 (src homology region 3) domains, three functional genes were identified from a fetal brain cDNA library, *SH3GL1*, *SH3GL2*, and *SH3GL3*. These genes map at chromosomes 19p13.3, 9p22, and 15q24, respectively (27) and function in signal transduction, cytoskeleton and aggregation of huntingtin (29-31). In addition, 3 expressed *SH3GL* pseudogenes were identified that mapped by FISH to chromosome 17 (Figure 3)(27). It will be important to characterize the expression of the other paralogous loci, *WI-9461*, *stSG31654*, *stSG40093*, and *WI-12393*, at each of the NF1REPs. Although these loci were originally isolated as ESTs expressed in multiple tissues (Unigene: www.ncbi.nlm.nih.gov/UniGene/index.html), it is unclear if each paralogous locus in NF1REP-P, -M, and -D is expressed and whether they represent pseudogenes, functional loci, or residual gene fragments.

NF1REP-mediated recombination

We propose that a high degree of homology between NF1REP-P and -M facilitates homologous recombination during meiosis or mitosis resulting in the deletion of intervening sequences. Consistent with this hypothesis, pseudogenes *SH3GLP1* and -2 are 97.8% identical, whereas *SH3GLP3* shares only 90% identity with either these (27). Further analysis of the identity between NF1REP-P and -M will require completing the sequence of the NF1REP-M domain; partial sequence analysis shows >98% identity (M. Dorschner, unpublished data). Recombination between the direct repeats NF1REP-P and -M could give rise to *NF1* microdeletions by either unequal recombination between sister chromatids or intrachromosomal recombination via a fold-back loop and excision. Distinguishing between these mechanisms will require further analyses to determine if NF1REP-mediated recombination is associated with a meiotic crossover event. The apparent preference for *de novo NF1* microdeletion of the maternally-derived chromosomes may provide a clue. Other REP-mediated rearrangements show a sex-dependent mechanism with maternally-derived deletions resulting from excision of an intrachromatid loop (32). Although in other cases, microdeletions mediated by flanking REP domains appear to arise by both mechanisms (33-35). If unequal meiotic recombination between sister chromatids underlies *NF1* microdeletion, it would predict the formation of a reciprocal duplication derivative. Whether a 1.5 Mb *NF1* duplication product would be stable is unknown; it may quickly undergo recombination and "revert" to a deletion (36). Non-mosaic trisomy 17 has not been reported in a live born and partial 17p or 17q trisomy is rare and even mosaic cases are uncommon (37), suggesting that many such rearrangements are lethal.

Patterns of REP domains and chromosomal rearrangements

About 10 years ago it became clear that intragenic, or relatively small, deletions, duplications, and inversions of the human genome could be mediated by homologous recombination between tandem genes, or other nearby repetitive sequences. Such rearrangements have been well described for the steroid sulfatase, α -globin, Factor VIII, *LDL* receptor, and other genes (reviewed in 36,38). Recently, however, the breakpoints of large contiguous gene deletions and duplications from 1-5 Mb in length were mapped to flanking repetitive sequences of high identity. Such low copy repetitive elements have been designated as REPs, duplicons, or paralogous regions (39,40). There is compelling evidence that homologous recombination between REPs is the molecular basis for a number of disorders (Table 5, reviewed in 26,38). The precedence was established for the neuropathies Charcot-Marie-Tooth type 1A (CMT1A) and hereditary neuropathy

with liability to pressure palsies (HNPP). Unequal recombination between flanking REPs during meiosis I results in duplication (CMT1A) or deletion (HNPP) of a 1.5 Mb segment of chromosome 17p11.2 (41,42). The two 24 kb CMT1A-REPs have 98.7% identity with an internal 557 bp recombination hotspot where 21 of 23 breakpoints occurred (43).

Although the characterization of REPs flanking large contiguous gene rearrangements is in its infancy, variability in REP length, number, complexity, and orientation is apparent. REP length varies considerably (Table 5) and may correlate directly with the size of the intervening deletion/duplication. This suggests that recombination between distant REPs may require longer tracts of identity for efficient pairing (26). Although a single CMT1A-REP lies on each side of the CMT1A/HNPP rearrangement, the number of REPs and the apparent preference for recombination between specific REPs can vary considerably. Three SMS-REPs are found in the 17p11.2 region, yet nearly all SMS (Smith-Magenis syndrome) deletions are due to crossover events between the proximal and distal REPs (44). The identification of eight REPs at 22q11 suggests that recombination between specific REP pairs may account for different rearrangements underlying multiple congenital anomaly disorders that map to this chromosomal region, such as velo-cardio-facial syndrome/DiGeorge syndrome (VCFS/DGS) and cat eye syndrome (CES) (45). REP domains may be very complex repeats that include multiple subrepeats, which can be in tandem or interspersed, inverted or direct in orientation (46-48). REPs may even be dispersed among chromosomes; FISH experiments suggest that copies of the PWS/AS (Prader-Willi syndrome/Angelman syndrome) REP may be at 15q24 and 16p11 (49). The apparent preference for REP domains to occur near the centromere of chromosomes (Table 5)(26) is consistent with reports of a strong bias for these regions to acquire paralogous segments. This phenomenon is referred to as pericentromeric plasticity and presumably accounts for the varied *NF1*-related fragments that are scattered among the centromeric regions of 7 different autosomes (50, reviewed in 39). Homologous recombination events and the resulting chromosomal rearrangements are also dependent upon the orientation of the repetitive sequences involved. For example, recombination between direct CMT1A-REPs results in deletion and duplication via unequal crossing over between chromatids (reviewed in 51), while recombination between indirect duplicons can result in either deletions or inversions (52-54).

Unique pathological aspects of NF1REP-mediated recombination

Several aspects of *NF1* microdeletions are unique among REP-mediated contiguous gene rearrangements in the human genome. For other disorders, REP-mediated rearrangements commonly account for a large fraction of analyzed cases. For example, >98% of CMT1A cases are caused by a duplication that results in partial trisomy of the 17p11.2 region that includes the *PMP22* locus, while <2% are due to missense mutations in the *PMP22* gene itself (55). In Angelman syndrome, large maternal deletions account for 70% of cases, uniparental disomy and imprinting mutations for additional 5%, and inactivating mutations in *UBE3A* for another 5% (56). In marked contrast, only 2-13% of *NF1* cases result from *NF1* microdeletions (16,18,57,58), while over 70% result from intragenic mutations that predict premature truncation of neurofibromin (8). Understanding why microdeletion is not the prevalent mutational mechanism may reveal important parameters that affect the efficiency of REP-mediated rearrangements. Perhaps the size and sequence identity of *NF1*/REP-P and -M are comparatively less than those of other genomic disorders, thereby reducing the probability of *NF1*/REP pairing. Or, polymorphism in the number and orientation of, or identity between, NF1REPs may result in a haplotype that is recombination-prone. A precedent for an inversion polymorphism mediated by flanking repetitive repeats has been established (54).

Our data suggest that *NF1* microdeletion may also predispose patients to the development of malignant tumors. This hypothesis is supported by our observation that 2 of the 17 (11%) unrelated microdeletion patients had a neurofibrosarcoma (Table 4, UWA124-3, UWA155-1). This clearly is greater than the expected occurrence of 1.4-3.5% in *NF1* patients (21,59), more so given the young age of the microdeletion patients. In addition, first degree affected relatives of 2 microdeletion patients died of malignancies (Table 4, UWA155-1, UWA169-1). Further studies are needed to confirm this hypothesis and to determine if this effect is mediated by the same putative gene that causes early onset of benign neurofibromas. Two lines of evidence suggest that the increased burden of cutaneous neurofibromas in deletion patients would be an unlikely cause of an apparent increased frequency of malignancy. First, cutaneous neurofibromas do not undergo malignant transformation; in cases where neurofibrosarcomas are associated with a neurofibroma it is either a plexiform neurofibroma or a neurofibroma involving a large nerve or nerve plexus (60). Second, the malignancies of the affected first degree relatives of our patients were CNS and fibrosarcoma, not neurofibrosarcoma (Table 4).

NF1REP-P and -M-mediated deletion in early embryogenesis may be an underlying mechanism of somatic mosaicism of *NF1*. It has been proposed that somatic mosaicism may be common among NF1 patients and could explain, for example, cases of a mildly affected parent with a severely affected child (61,62). Patients with somatic mosaicism for an *NF1* deletion have been described (16,57,63-65). Because breakpoints were not mapped in these cases, it is not known whether these deletions involved the entire *NF1* gene and/or contiguous genes. The frequency of somatic mosaicism for an *NF1* deletion was estimated at 1.5% (16,57). However, this may be underestimated significantly due to the low detection rate of the methods employed.

This is the first report of a REP-mediated rearrangement resulting in the loss of a tumor suppressor gene. Therefore, in addition to the germline rearrangements reported here, NF1REP-mediated somatic recombination could be an important mechanism for the loss of heterozygosity (LOH) at *NF1* in tumors of NF1 patients (5,7,66,67). This hypothesis is consistent with our recent analysis of LOH at *NF1* in primary leukemic cells of children affected with NF1 that developed malignant myeloid disorders (Stephens et al., unpublished data). LOH in 2 of 20 tumors arose by an interstitial deletion of a 1-2 Mb segment comparable to the germline deletions described here. Additional informative polymorphisms are needed to determine if the deletion breakpoints are at NF1REP-P and -M. Other examples of clustered neoplasia-related rearrangements could also result from a REP-mediated recombination mechanism. For example, the interstitial 20q deletion in polycythemia vera and myeloid malignancies (54) and the i(17q)-associated hematologic malignancies (68).

The precocious neurofibromagenesis and severe tumor burden of patients with *NF1* microdeletions is consistent with our hypothesis that deletion of a gene or regulatory sequence, in conjunction with neurofibromin haploinsufficiency, potentiates development of neurofibromas. All of the deletion patients showed either childhood onset and/or large numbers of cutaneous neurofibromas (Figure 2, Table 4), with the exception of UWA166-3 who is only 4 years old. Patient UWA113-1 has the smallest deletion of about 1 Mb, thereby establishing a critical interval between *FB12A2* and *SH3GLP1* as the location of the putative tumor-promoting gene (Figure 2). These data excluded the strong candidate gene *KSR*, kinase suppressor of ras (69). Currently, the critical region is known to harbor 4 genes, *NF1*, *OMG*, *EVI2A*, *EVI2B*, 2 pseudogenes, and 7 ESTs (Figure 2, Table 3). The products of these genes are not strong candidates for potentiating neurofibromagenesis. *OMG*, *EVI2A*, and *EVI2B* are genes of unknown function located entirely within intron 27b of the *NF1* gene, but they are transcribed from the opposite direction. *OMG* encodes a glycoprotein, OMgp, which is expressed only in the central nervous system in neurons and oligodendrocytes, and is displayed in CNS myelin (70,71). Although growth suppression of NIH3T3 fibroblasts overexpressing OMgp suggests it plays a role in cell proliferation (72), its lack of expression in the peripheral nervous system makes it a poor candidate. *EVI2A* and *-B* genes are more widely expressed and predict a putative transmembrane protein of unknown function (73); it is not known if they are expressed in Schwann cells, which appear to be the progenitor cell of a neurofibroma (11). *EVI2A* and *-B* are human orthologs of mouse loci where retroviral integration causes myeloid leukemia. Further investigation, however, revealed that it was inactivation of *NF1*, not the *EVI2* genes, that caused the leukemia (74). The identification of patients deleted for *OMG*, *EVI2A*, *EVI2B* or a segment of *NF1* along with flanking sequences would be a direct test of a role for these genes in the early onset of neurofibromas. Assuming exclusion of *NF1* and the embedded genes, the critical region is reduced to ~ 700 kb in length. The 7 ESTs that we mapped to this region, and the sequence-ready contig will provide the basis for identifying and characterizing the putative tumor-modifying gene.

MATERIALS AND METHODS

Subjects. Patients described previously include UWA106-3 (12,13), UWA69-3, UWA119-1, UWA123-3, and UWA128-3 (13), UWA166-2 and UWA169-1 (19), UWA147-3, UWA156-1, UWA160-1, UWA167-1, UWA172-1, and UWA176-1 (K. Maruyama et al., submitted). Table 4 includes clinical findings from these reports and more recent clinical evaluations. This study was approved by the Institutional Review Boards of the University of Washington and Children's Hospital and Regional Medical Center, Seattle, WA. Immortalized cell lines and human/rodent somatic cell hybrid lines carrying a single human chromosome 17 were constructed as described previously (13).

BAC library screening. Marker loci were amplified in the presence of ^{32}P -dCTP as described previously (<http://www.sanger.ac.uk>). A cocktail of probes, 1×10^6 - 10^7 cpm/ml hybridization solution each, was used to screen the RPCI-11 human BAC library, segment 4 (BACPAC Resources, Buffalo, NY, <http://bacpac.med.buffalo.edu>) by hybridization. Membranes were prehybridized in 25 ml of hybridization buffer (75) at 65°C for one hour, hybridized

overnight, and washed 4-6 times at increasing stringency, with a final wash of 0.2X SSC/0.1% SDS for 45 minutes. Following autoradiography for 1-2 days at -70°C with intensifying screens, positive clone addresses were determined and obtained from BACPAC resources. BAC DNA was isolated from 3 ml overnight cultures using the Qiagen Spin miniprep plasmid kit (Qiagen, Chatsworth, CA) according to the manufacturer's directions.

STSs, ESTs and generation of new markers. Loci were amplified either as described in the database entry or using a program with an initial denaturation of 94°C for 2 minutes, followed by 35 cycles of 94°C for 15 seconds, 59°C for 15 seconds, and 72°C for 60 seconds, and a final extension of 8 minutes. Primers for the amplification of *D17S117* and *D17S120* were designed from partial sequence analysis of plasmid clones. *D17S117* was amplified with primers 5'-AGGATGGACTAGGATTCTTAGTG-3' and 5'-GCTGTCAATCACCAAAGTCGAG-3' for *D17S117*. *D17S120* were amplified with primers 5'-CTCGAAGGTAGGATAGTGACAG-3' and 5'-GATAGTTTGAGCTCAGGAATGTG-3'.

New markers were developed from the ends of BAC clone inserts. DNA was extracted from 300 ml of overnight culture from selected BAC clones using the Qiagen MIDI prep plasmid kit (Qiagen, Chatsworth, CA). BAC end termini were sequenced using 0.8-1.0 µg of purified BAC DNA, T7 or SP6 primers, and BigDye terminator chemistry (ABI, Foster City, CA). Nucleotide sequences were analyzed with Sequencher 3.0 (Gene Codes, Ann Arbor, MI) and primers were designed (Table 2).

ACKNOWLEDGEMENTS

We thank the NF1 patients and their families for their continued cooperation. This research was supported by the Department of the Army, U.S. Army Medical Research and Materiel Command grant NF960043 awarded to K.S.

REFERENCES

1. Martin, G.A., Viskochil, D., Bollag, G., McCabe, P.C., Crosier, W.J., Haubruck, H., Conroy, L., Clark, R., O'Connell, P., Cawthon, R.M., and et al. (1990) The GAP-related domain of the neurofibromatosis type 1 gene product interacts with ras p21. *Cell* 63, 843-849.
2. Feldkamp, M.M., Angelov, L., and Guha, A. (1999) Neurofibromatosis type 1 peripheral nerve tumors: aberrant activation of the Ras pathway. *Surg. Neurol.*, 51, 211-218.
3. Bollag, G., Clapp, D.W., Shih, S., Adler, F., Zhang, Y.Y., Thompson, P., Lange, B.J., Freedman, M.H., McCormick, F., Jacks, T., and Shannon, K. (1996) Loss of NF1 results in activation of the Ras signaling pathway and leads to aberrant growth in haematopoietic cells. *Nature Genet.*, 12, 144-148.
4. Zhang, Y.Y., Vik, T.A., Ryder, J.W., Srour, E.F., Jacks, T., Shannon, K., and Clapp, D.W. (1998) Nf1 regulates hematopoietic progenitor cell growth and ras signaling in response to multiple cytokines. *J. Exp. Med.*, 187, 1893-1902.
5. Sawada, S., Florell, S., Purandare, S.M., Ota, M., Stephens, K., and Viskochil, D. (1996) Identification of NF1 mutations in both alleles of a dermal neurofibroma. *Nature Genet.*, 14, 110-112.
6. Serra, E., Puig, S., Otero, D., Gaona, A., Kruyer, H., Ars, E., Estivill, X., and Lazaro, C. (1997) Confirmation of a double-hit model for the NF1 gene in benign neurofibromas. *Am. J. Hum. Genet.*, 61, 512-519.
7. Side, L., Taylor, B., Cayouette, M., Conner, E., Thompspon, P., Luce, M., and Shannon, K. (1997) Homozygous inactivation of the NF1 gene in bone marrow cells from children with neurofibromatosis type 1 and malignant myeloid disorders. *N. Engl. J. Med.*, 336, 1713-1720.
8. Park, V.M., and Pivnick, E.K. (1998) Neurofibromatosis type 1 (NF1): a protein truncation assay yielding identification of mutations in 73% of patients. *J. Med. Genet.*, 35, 813-820.
9. Riccardi, V.M. (1993) Molecular biology of the neurofibromatoses. *Semin. Dermatol.*, 12, 266-273.
10. Gutmann, D.H., Aylsworth, A., Carey, J.C., Korf, B., Marks, J., Pyeritz, R.E., Rubenstein, A., and Viskochil, D. (1997) The diagnostic evaluation and multidisciplinary management of neurofibromatosis 1 and neurofibromatosis 2. *J.A.M.A.*, 278, 51-57.

11. Kluwe, L., Friedrich, R., and Mautner, V.F. (1999) Loss of NF1 allele in Schwann cells but not in fibroblasts derived from an NF1-associated neurofibroma. *Genes Chromosomes Cancer* **24**, 283-285.
12. Kayes, L.M., Riccardi, V.M., Burke, W., Bennett, R.L., and Stephens, K. (1992) Large de novo DNA deletion in a patient with sporadic neurofibromatosis 1, mental retardation, and dysmorphism. *J. Med. Genet.*, **29**, 686-690.
13. Kayes, L.M., Burke, W., Riccardi, V.M., Bennett, R., Ehrlich, P., Rubenstein, A., and Stephens, K. (1994) Deletions spanning the neurofibromatosis 1 gene: identification and phenotype of five patients. *Am. J. Hum. Genet.*, **54**, 424-436.
14. Leppig, K.A., Viskochil, D., Neil, S., Rubenstein, A., Johnson, V.P., Zhu, X.L., Brothman, A.R., and Stephens, K. (1996) The detection of contiguous gene deletions at the neurofibromatosis 1 locus with fluorescence in situ hybridization. *Cytogenet. Cell Genet.*, **72**, 95-98.
15. Wu, B.-L., Austin, M., Schneider, G., Boles, R., and Korf, B. (1995) Deletion of the entire NF1 gene detected by FISH: four deletion patients associated with severe manifestations. *Am. J. Med. Genet.*, **59**, 528-535.
16. Ainsworth, P.J., Chakraborty, P.K., and Weksberg, R. (1997) Example of somatic mosaicism in a series of de novo neurofibromatosis type 1 cases due to a maternally derived deletion. *Hum. Mutation* **9**, 452-457.
17. Cnossen, M.H., van der Est, M.N., Breuning, H., van Asperen, C.J., Breslau-Siderius, E.J., van der Ploeg, A.T., de Goede-Bolder, A., van den Ouweland, A.M.W., Halley, D.J.J., and Niermeijer, M.F. (1997) Deletions spanning the neurofibromatosis type 1 gene: implications for genotype-phenotype correlations in neurofibromatosis type 1? *Hum. Mutation* **9**, 458-464.
18. Valero, M.C., Pascual Castroviejo, I., Velasco, E., Moreno, F., and Hern'andez Chico, C. (1997) Identification of de novo deletions at the NF1 gene: no preferential paternal origin and phenotypic analysis of patients. *Hum. Genet.*, **99**, 720-726.
19. Leppig, K., Kaplan, P., Viskochil, D., Weaver, M., Orterberg, J., and Stephens, K. (1997) Familial neurofibromatosis 1 gene deletions: cosegregation with distinctive facial features and early onset of cutaneous neurofibromas. *Am. J. Med. Genet.*, **73**, 197-204.
20. Wu, B.L., Schneider, G.H., and Korf, B.R. (1997) Deletion of the entire NF1 gene causing distinct manifestations in a family. *Am. J. Med. Genet.*, **69**, 98-101.
21. Huson, S., Harper, P., and Compston, D. (1988) Von Recklinghausen neurofibromatosis: a clinical and population study in south-east Wales. *Brain* **111**, 1355-1381.
22. Huson, S.M. (1994) In Huson, S.M., and Hughes, R.A.C., (ed.), *The Neurofibromatoses: a pathogenetic and clinical overview*. Chapman and Hall Medical, London, , first Ed., pp. 160-203
23. Marchuk, D.A., Tavakkol, R., Wallace, M.R., Brownstein, B.H., Taillon Miller, P., Fong, C.T., Legius, E., Andersen, L.B., Glover, T.W., and Collins, F.S. (1992) A yeast artificial chromosome contig encompassing the type 1 neurofibromatosis gene. *Genomics* **13**, 672-680.
24. Shannon, K.M., P, O.C., Martin, G.A., Paderanga, D., Olson, K., Dinndorf, P., and McCormick, F. (1994) Loss of the normal NF1 allele from the bone marrow of children with type 1 neurofibromatosis and malignant myeloid disorders. *N. Engl. J. Med.*, **330**, 597-601.
25. Shen, S., Battersby, S., Weaver, M., Clark, E., Stephens, K., and Harmar, A.J. (1999) Refined mapping of the human serotonin transporter (SLC6A4) gene within 17q11 adjacent to the CPD and NF1 genes. *Eur. J. Hum. Genet.*, in press.
26. Lupski, J.R. (1998) Genomic disorders: structural features of the genome can lead to DNA rearrangements and human disease traits. *Trends Genet.*, **14**, 417-422.
27. Giachino, C., Lantelme, E., Lanzetti, L., Saccone, S., Bella Valle, G., and Migone, N. (1997) A novel SH3-containing human gene family preferentially expressed in the central nervous system. *Genomics* **41**, 427-434.
28. Kaplan, P., and Rosenblatt, B. (1985) A distinctive facial appearance in neurofibromatosis von Recklinghausen. *Am. J. Med. Genet.*, **21**, 463-470.
29. Mayer, B.J., and Gupta, R. (1998) Functions of SH2 and SH3 domains. *Curr. Top. Microbiol. Immunol.*, **228**, 1-22.

30. Sittler, A., Walter, S., Wedemeyer, N., Hasenbank, R., Scherzinger, E., Eickhoff, H., Bates, G.P., Lehrach, H., and Wanker, E.E. (1998) SH3GL3 associates with the huntingtin exon 1 protein and promotes the formation of polyglutamine-containing protein aggregates. *Mol. Cell* **2**, 427-436.
31. So, C.W., Caldas, C., Liu, M.M., Chen, S.J., Huang, Q.H., Gu, L.J., Sham, M.H., Wiedemann, L.M., and Chan, L.C. (1997) EEN encodes for a member of a new family of proteins containing an Src homology 3 domain and is the third gene located on chromosome 19p13 that fuses to MLL in human leukemia. *Proc Natl Acad Sci USA* **94**, 2563-2568.
32. Lopes, J., Ravise, N., Vandenberghe, A., Palau, F., Ionasescu, V., Mayer, M., Levy, N., Wood, N., Tachi, N., Bouche, P., Latour, P., Ruberg, M., Brice, A., and LeGuern, E. (1998) Fine mapping of de novo CMT1A and HNPP rearrangements within CMT1A-REPs evidences two distinct sex-dependent mechanisms and candidate sequences involved in recombination. *Hum. Mol. Genet.* **7**, 141-148.
33. Dutly, F., and Schinzel, A. (1996) Unequal interchromosomal rearrangements may result in elastin gene deletions causing the Williams-Beuren syndrome. *Hum. Mol. Genet.* **5**, 1893-1898.
34. Carrozzo, R., Rossi, E., Christian, S.L., Kittikamron, K., Livieri, C., Corrias, A., Pucci, L., Fois, A., Simi, P., Bosio, L., Beccaria, L., Zuffardi, O., and Ledbetter, D.H. (1997) Inter- and intrachromosomal rearrangements are both involved in the origin of 15q11-q13 deletions in Prader-Willi syndrome. *Am. J. Hum. Genet.* **61**, 228-231.
35. Baumer, A., Dutly, F., Balmer, D., Riegel, M., Tukel, T., Krajewska-Walasek, M., and Schinzel, A.A. (1998) High level of unequal meiotic crossovers at the origin of the 22q11.2 and 7q11.23 deletions. *Hum. Mol. Genet.* **7**, 887-894.
36. Cooper, D.N., Krawczak, M., and Antonarakis, S.E. (1995) In Scriver, C.R., Beaudet, A.L., Sly, W.S., and Valle, D., (ed.), *The metabolic and molecular bases of inherited disease*. McGraw-Hill, Inc., New York, Vol. 1, 7 Ed., pp. 259-292.
37. Lenzini, E., Leszl, A., Artifoni, L., Casellato, R., Tenconi, R., and Baccichetti, C. (1988) Partial duplication of 17 long arm. *Ann Genet* **31**, 175-180.
38. Mazzarella, R., and Schlessinger, D. (1998) Pathological consequences of sequence duplications in the human genome. *Genome Res.* **8**, 1007-1021.
39. Eichler, E.E. (1998) Masquerading repeats: paralogous pitfalls of the human genome. *Genome Res.* **8**, 758-762.
40. Reiter, L.T., Murakami, T., Koeuth, T., Pentao, L., Muzny, D.M., Gibbs, R.A., and Lupski, J.R. (1996) A recombination hotspot responsible for two inherited peripheral neuropathies is located near a *mariner* transposon-like element. *Nature Genet.* **12**, 288-297.
41. Reiter, L.T., Hastings, P.J., Nelis, E., De Jonghe, P., Van Broeckhoven, C., and Lupski, J.R. (1998) Human meiotic recombination products revealed by sequencing a hotspot for homologous strand exchange in multiple HNPP deletion patients. *Am. J. Hum. Genet.* **62**, 1023-1033.
42. Chance, P.F., Abbas, N., Lensch, M.W., Pentao, L., Toa, B.B., Patel, P.I., and Lupski, J.R. (1994) Two autosomal dominant neuropathies result from reciprocal DNA duplication/deletion of a region on chromosome 17. *Hum. Mol. Genet.* **3**, 223-228.
43. Reiter, L.T., Murakami, T., Koeuth, T., Gibbs, R.A., and Lupski, J.R. (1997) The human COX10 gene is disrupted during homologous recombination between the 24 kb proximal and distal CMT1A-REPs. *Hum. Mol. Genet.* **6**, 1595-1603.
44. Chen, K.-S., Manian, P., Koeuth, T., Potocki, L., Zhao, Q., Chinault, A.C., Lee, C.C., and Lupski, J.R. (1997) Homologous recombination of a flanking repeat gene cluster is a mechanism for a common contiguous gene deletion syndrome. *Nature Genet.* **17**, 154-163.
45. Edelmann, L., Pandita, R.K., Spiteri, E., Funke, B., Goldberg, R., Palanisamy, N., Chaganti, R.S., Magenis, E., Shprintzen, R.J., and Morrow, B.E. (1999) A common molecular basis for rearrangement disorders on chromosome 22q11. *Hum. Mol. Genet.* **8**, 1157-1167.
46. Amos-Landgraf, J.M., Ji, Y., Gottlieb, W., Depinet, T., Wandstrat, A.E., Cassidy, S.B., Driscoll, D.J., Rogan, P.K., Schwartz, S., and Nicholls, R.D. (1999) Chromosome breakage in the Prader-Willi and Angelman syndromes involves recombination between large, transcribed repeats at proximal and distal breakpoints. *Am. J. Hum. Genet.* **65**, 370-386.

47. Perez Jurado, L.A., Peoples, R., Kaplan, P., Hamel, B.C., and Francke, U. (1996) Molecular definition of the chromosome 7 deletion in Williams syndrome and parent-of-origin effects on growth. *Am. J. Hum. Genet.*, **59**, 781-792.
48. Edelmann, L., Pandita, R.K., and Morrow, B.E. (1999) Low-Copy Repeats Mediate the Common 3-Mb Deletion in Patients with Velo- cardio-facial Syndrome. *Am. J. Hum. Genet.*, **64**, 1076-1086.
49. Christian, S.L., Fantes, J.A., Mewborn, S.K., Huang, B., and Ledbetter, D.H. (1999) Large genomic duplicons map to sites of instability in the prader- Willi/Angelman syndrome chromosome region (15q11-q13). *Hum. Mol. Genet.*, **8**, 1025-1037.
50. Regnier, V., Meddeb, M., Lecointre, G., Richard, F., Duverger, A., Nguyen, V.C., Dutrillaux, B., Bernheim, A., and Dangelot, G. (1997) Emergence and scattering of multiple neurofibromatosis (NF1)-related sequences during hominoid evolution suggest a process of pericentromeric interchromosomal transposition. *Hum. Mol. Genet.*, **6**, 9-16.
51. Lupski, J.R. (1999) Charcot-Marie-Tooth polyneuropathy: duplication, gene dosage, and genetic heterogeneity. *Pediatr. Res.*, **45**, 159-165.
52. Konrad, M., Saunier, S., Heidet, L., Silbermann, F., Benessy, F., Calado, J., Le Paslier, D., Broyer, M., Gubler, M.C., and Antignac, C. (1996) Large homozygous deletions of the 2q13 region are a major cause of juvenile nephronophthisis. *Hum. Mol. Genet.*, **5**, 367-371.
53. Nothwang, H.G., Stubanus, M., Adolphs, J., Hanusch, H., Vossmerbaumer, U., Denich, D., Kubler, M., Mincheva, A., Lichter, P., and Hildebrandt, F. (1998) Construction of a gene map of the nephronophthisis type 1 (NPHP1) region on human chromosome 2q12-q13. *Genomics* **47**, 276-285.
54. Small, K., Iber, J., and Warren, S.T. (1997) Emerin deletion reveals a common X-chromosome inversion mediated by inverted repeats. *Nat Genet* **16**, 96-99.
55. Bird, T. (1999) Charcot-Marie-Tooth Type 1. GeneClinics Web site. Available at <http://www.geneclinics.org>. Accessed August 15, 1999.
56. Moncla, A., Malzac, P., Livet, M.O., Voelckel, M.A., Mancini, J., Delaroziere, J.C., Philip, N., and Mattei, J.F. (1999) Angelman syndrome resulting from UBE3A mutations in 14 patients from eight families: clinical manifestations and genetic counselling. *J. Med. Genet.*, **36**, 554-560.
57. Rasmussen, S.A., Colman, S.D., Ho, V.T., Abernathy, C.R., Arn, P.H., Weiss, L., Schwartz, C., Saul, R.A., and Wallace, M.R. (1998) Constitutional and mosaic large NF1 gene deletions in neurofibromatosis type 1. *J. Med. Genet.*, **35**, 468-471.
58. Upadhyaya, M., Ruggieri, M., Maynard, J., Osborn, M., Hartog, C., Mudd, S., Penttinen, M., Cordeiro, I., Ponder, M., Ponder, B.A., Krawczak, M., and Cooper, D.N. (1998) Gross deletions of the neurofibromatosis type 1 (NF1) gene are predominantly of maternal origin and commonly associated with a learning disability, dysmorphic features and developmental delay. *Hum. Genet.*, **102**, 591-597.
59. Riccardi, V.M., and Powell, P.P. (1989) Neurofibrosarcoma as a complication of von Recklinghausen neurofibromatosis. *Neurofibromatosis* **2**, 152-165.
60. Woodruff, J.M. (1999) Pathology of tumors of the peripheral nerve sheath in type 1 neurofibromatosis. *Am J Med Genet (Semin Med Genet)* **89**, 23-30.
61. Riccardi, V.M. (1993) Genotype, malleotype, phenotype, and randomness: lessons from neurofibromatosis-1 (NF-1). *Am. J. Hum. Genet.*, **53**, 301-304.
62. Zlotogora, J. (1993) Mutations in von Recklinghausen neurofibromatosis: an hypothesis. *Am. J. Med. Genet.*, **46**, 182-184.
63. Colman, S.D., Rasmussen, S.A., Ho, V.T., Abernathy, C.R., and Wallace, M.R. (1996) Somatic mosaicism in a patient with neurofibromatosis type 1. *Am. J. Hum. Genet.*, **58**, 484-490.
64. Tonsgard, J.H., Yelavarthi, K.K., Cushner, S., Short, M.P., and Lindgren, V. (1997) Do NF1 gene deletions result in a characteristic phenotype? *Am. J. Med. Genet.*, **73**, 80-86.
65. Wu, B.L., Boles, R.G., Yaari, H., Weremowicz, S., Schneider, G.H., and Korf, B.R. (1997) Somatic mosaicism for deletion of the entire NF1 gene identified by FISH. *Hum. Genet.*, **99**, 209-213.

66. Xu, W., Mulligan, L.M., Ponder, M.A., Liu, L., Smith, B.A., Mathew, C.G., and Ponder, B.A. (1992) Loss of NF1 alleles in pheochromocytomas from patients with type I neurofibromatosis. *Genes Chromosomes Cancer* 4, 337-342.
67. Lothe, R.A., Slettan, A., Saeter, G., Brogger, A., Borresen, A.L., and Nesland, J.M. (1995) Alterations at chromosome 17 loci in peripheral nerve sheath tumors. *J. Neuropathol. Exp. Neurol.* 54, 65-73.
68. Fioretos, T., Strombeck, B., Sandberg, T., Johansson, B., Billstrom, R., Borg, A., Nilsson, P.G., Van Den Berghe, H., Hagemeijer, A., Mitelman, F., and Hoglund, M. (1999) Isochromosome 17q in blast crisis of chronic myeloid leukemia and in other hematologic malignancies is the result of clustered breakpoints in 17p11 and is not associated with coding TP53 mutations. *Blood* 94, 225-232.
69. Cacace, A.M., Michaud, N.R., Therrien, M., Mathes, K., Copeland, T., Rubin, G.M., and Morrison, D.K. (1999) Identification of constitutive and ras-inducible phosphorylation sites of KSR: implications for 14-3-3 binding, mitogen-activated protein kinase binding, and KSR overexpression. *Mol. Cell Biol.* 19, 229-240.
70. Habib, A.A., Marton, L.S., Allvardt, B., Gulcher, J.R., Mikol, D.D., Hognason, T., Chattopadhyay, N., and Stefansson, K. (1998) Expression of the oligodendrocyte-myelin glycoprotein by neurons in the mouse central nervous system. *J. Neurochem.* 70, 1704-1711.
71. Mikol, D.D., and Stefansson, K. (1988) A phosphatidylinositol-linked peanut agglutinin-binding glycoprotein in central nervous system myelin and on oligodendrocytes. *J. Cell Biol.* 106, 1273-1279.
72. Habib, A.A., Gulcher, J.R., Hognason, T., Zheng, L., and Stefansson, K. (1998) The OMgp gene, a second growth suppressor within the NF1 gene. *Oncogene* 16, 1525-1531.
73. Cawthon, R.M., Andersen, L.B., Buchberg, A.M., Xu, G.F., O'Connell, P., Viskochil, D., Weiss, R.B., Wallace, M.R., Marchuk, D.A., Culver, M., and et al. (1991) cDNA sequence and genomic structure of EV12B, a gene lying within an intron of the neurofibromatosis type 1 gene. *Genomics* 9, 446-460.
74. Largaespada, D.A., Shaughnessy, J.D., Jr., Jenkins, N.A., and Copeland, N.G. (1995) Retroviral integration at the Evi-2 locus in BXH-2 myeloid leukemia cell lines disrupts Nf1 expression without changes in steady-state Ras- GTP levels. *J. Virol.* 69, 5095-5102.
75. Church, G.M., and Gilbert, W. (1984) Genomic sequencing. *Proc Natl Acad Sci U S A* 81, 1991-1995.
76. van Tuinen, P., Rich, D.C., Summers, K.M., and Ledbetter, D.H. (1987) Regional mapping panel for human chromosome 17: application to neurofibromatosis type 1. *Genomics* 1, 374-381.
77. Ledbetter, D.H., Rich, D.C., P. O.C., Leppert, M., and Carey, J.C. (1989) Precise localization of NF1 to 17q11.2 by balanced translocation. *Am. J. Hum. Genet.* 44, 20-24.

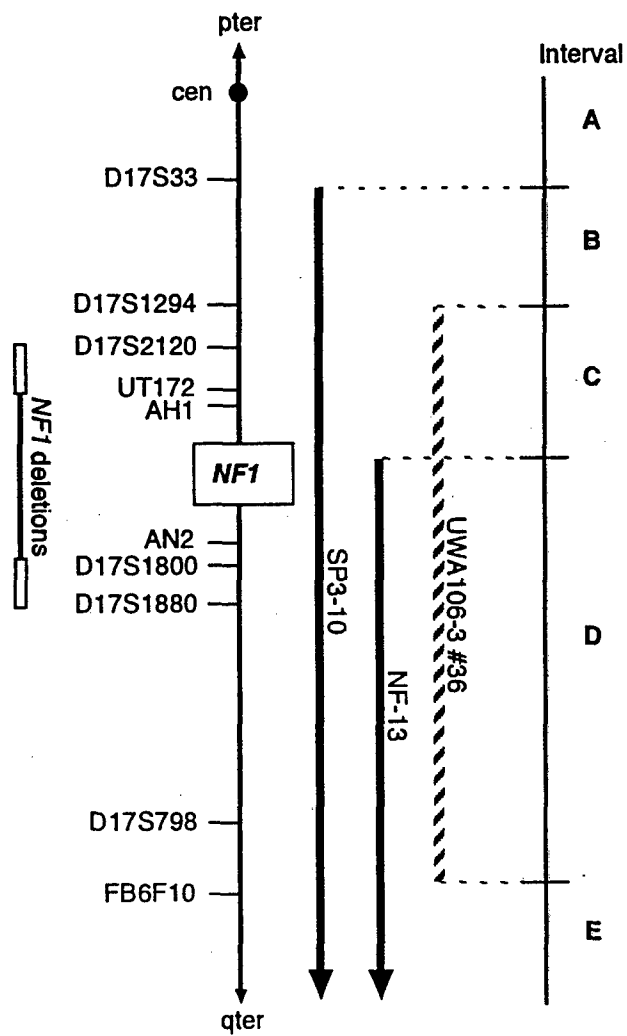
FIGURE LEGENDS

Figure 1. Hybrid mapping panel for *NF1* region. The location of markers in the *NF1* region are depicted, along with the *NF1* deletion previously defined in patients, with open bars representing the breakpoint cluster regions (K. Maruyama et al., submitted). Loci were mapped to one of five intervals, A through E, on chromosome 17 by their presence or absence in human/rodent somatic cell hybrid lines. The hybrid line UWA106-3-#36 was constructed from *NF1* microdeletion patient UWA106-3 and carries a chromosome 17 deleted for the indicated segment (13). Line SP3-10 carries human chromosome segment 17q11.2 to qter (76) and NF13 carries a segment from *NF1* intron 27b to qter (77).

Figure 2. Physical contig of the *NF1* region. The thick black bar is a schematic of the chromosome 17q11.2 region with STS loci placed above the bar and genes and EST loci below. The BAC, PAC, and YAC clones comprising the contig are shown above; open ellipses are aligned with the loci on the chromosome schematic and indicate a positive hit in the clone; sequenced BAC/PAC clones are indicated with an asterisk. Vertical bars at the ends of BACs represent insert termini that were sequenced and submitted to Genbank, but not converted to amplimers. Scale in Mb is at the top of the figure. The size and extent of microdeletions of *NF1* patients are shown below the chromosome. The common *NF1* deletion region was identified in 14 out of 17 unrelated patients; while 3 patients had novel deletions as shown. The open boxes represent flanking repetitive sequences (NF1REP) where the majority of breakpoints mapped.

Figure 3: NF1REP domains on chromosome 17. The locations of the three NF1REP regions, designated -P, -M, -D for proximal, medial, and distal are shown along with the 5 loci they are known to contain. In addition, the closest unique marker flanking each REP is indicated. The cross-hatched bar represents the 1.5 Mb region commonly deleted in *NF1* microdeletion patients.

FIGURE 1



A vertical scale with tick marks at 0, 1, 2, 3, and 4.

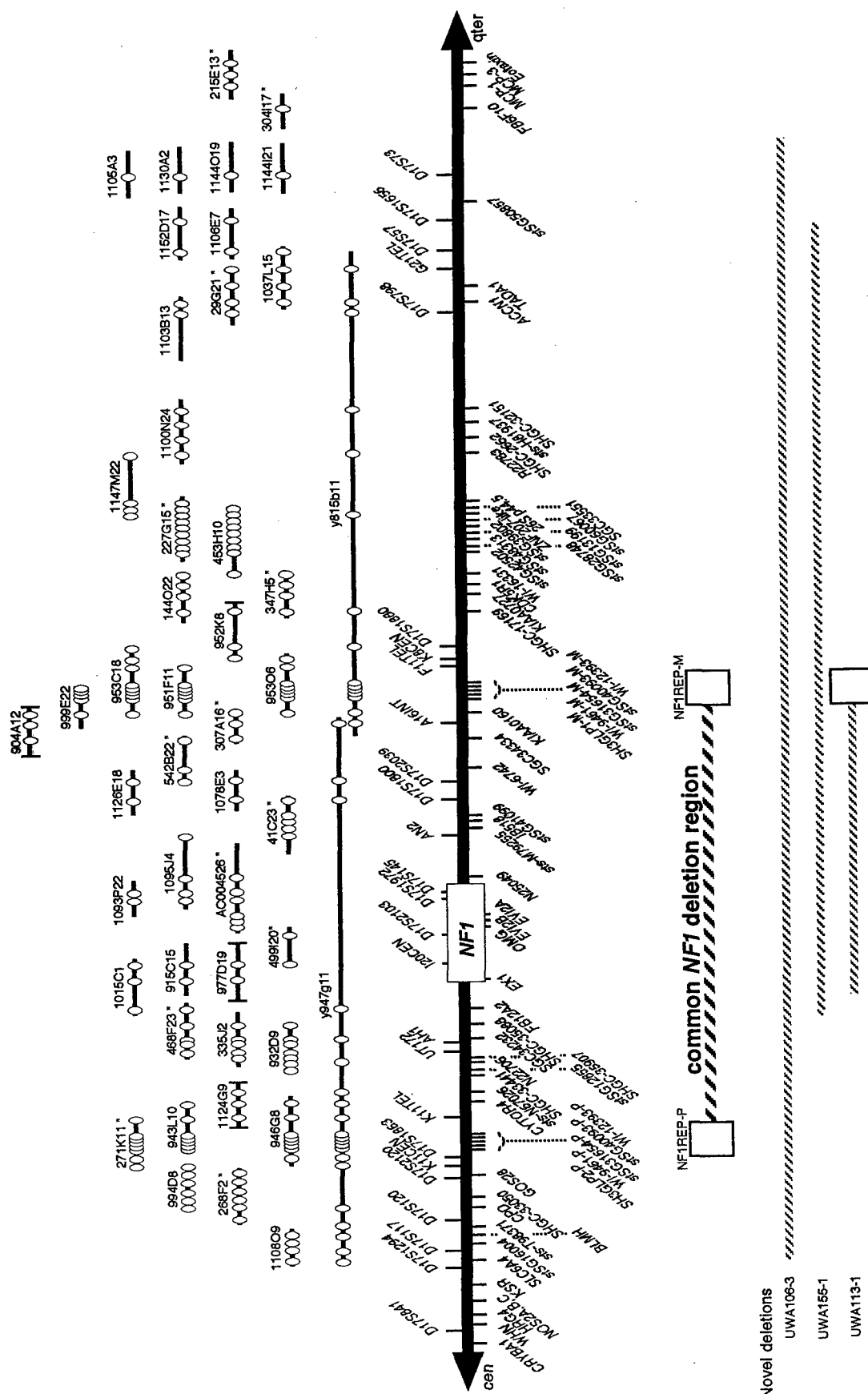


FIGURE 3

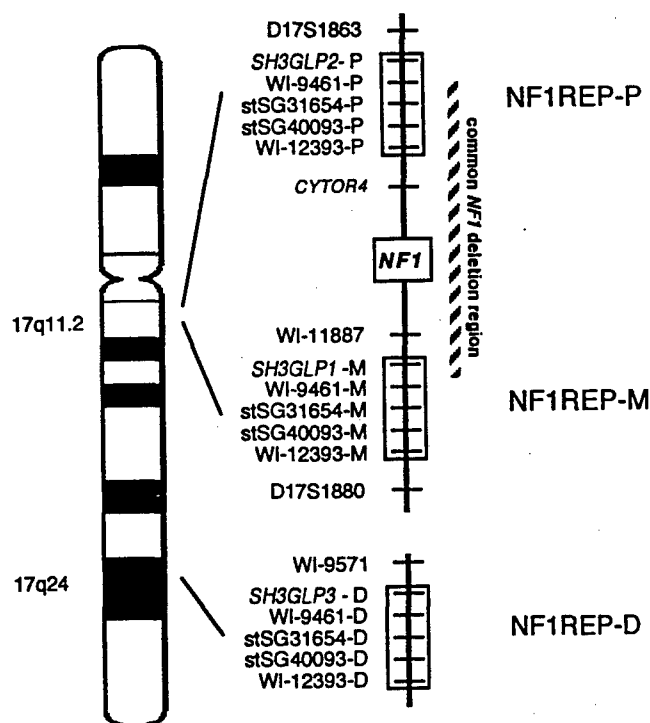


Table 1: BAC/PAC clones from 17q11.2

Clone source	Clone name	Genbank accession #	Size (kb)
hRPK	1108 O 9		
hRPK	268 F 2	AC006050	163
hRPK	994 D 8		
hRPK	946 G 8		
hRPK	271 K 11	AC005562	199
hRPK	943 L 10		
hRPK	1124 G 9		
hRPK	932 D 9		
hCIT	335 J 2		
hCIT	468 F 23	AC004666	120
hRPK	1015 C 1		
hRPK	915 C 15		
hRPK	997 D 19		
hCIT	499 I 20	AC004222	119
		AC004526 ^a	297
hRPK	1093 P 22		
hRPK	1095 J 4		
hCIT	41 C 23	AC003101	208
hRPK	1078 I 13		
hRPK	1126 E 16		
hCIT	542 B 22	AC004523	131
hCIT	307 A 16	AC003041	78
hRPK	904 A 12		
hRPK	999 E 22		
hRPK	953 O 6		
hRPK	951 F 11		
hRPK	953 C 18		
hRPC	144 O 22		
hRPK	952 K 8		
hCIT	347 H 5	AC002119	109
hCIT	453 H 10		
hRPK	227 G 15	AC005899	184
hRPK	1147 M 22		
hRPK	1100 N 24		
hRPK	1103 B 13		
hRPC	29 G 21	AC003687	141
hRPK	1037 L 15		
hRPK	1106 E 7		
hRPK	1152 D 17		
hRPK	1014 I 16		
hRPK	1144 I 21		
hRPK	1130 A 2		
hRPK	1105 A 3		
hCIT	304 I 17	AC004147	139
hRPK	215 E 13	AC005549	147

hRPK = clones from RPCI-11 Human Male BAC library

hCIT = clones from CITB Caltech Human BAC library

hRPC = clones from RPCI Human PAC library.

^acontiguous sequence of two overlapping BAC clones

Table 2: New BAC-end derived loci

Locus	Forward primer (5'-3')	Reverse primer (5'-3')	Size (bp)	Genbank accession #
F2-CEN	GCTGGAAGCCACATTGTCTG	GCACACAAATTCTTTGGGA	77	AC006050
F2-TEL	TCCCCITGCAGCATTGCTAT	CAGACACTTCTCCCCTCTACCCT	150	AC006050
K11-CEN	ACACTGCTGCTCTTCACCATTG	CCACCCATGAGCAAGTTCG	150	AC005562
K11-TEL	AGGTGTGAGCCACTGTGCACT	GGCTCCCCTAGGAAGCTCC	200	AC005562
I20-CEN	CGAACTCCTGACCTCGTGATC	ACCTGGTGTCTAGAGCTGATG	788	AC004222
F11-TEL	TGAGACTGATTGTAGCAGAAGTC	ACCTGTGGCTGTTGAACACTTG	325	AF170177
K8-CEN	GCTCCATGTTCCATGCTATGAG	TCTTCTCCACTCATTCTTTGTC	363	AF170179
G21-TEL	TTAGTTAGAGCCACCCCTCC	CCATAGGTGTGCTGGCCAC	155	AC003687
A16-INT	GGCCTCCAACCTGGTAGTCTG	GTCTGCAAATGAGCTGACAAGCT	320	AC004523

Table 3: Genes and ESTs involved in *NF1* microdeletions

Gene/EST	Description	Genbank Accession #	Unigene cluster	Gene/EST	Description	Genbank Accession #	Unigene cluster
<i>SLC6A4</i>	serotonin transporter	L05568	553	<i>sSG-41099</i>		H29300	7985
<i>sSG16004</i>		R96721	155925	<i>WI-6742</i>		R44280	8179
<i>BLMH</i>	bleomycin hydrolase	X92106	78943	<i>SHGC-34334</i>		D19683	30670
<i>sts-T98371</i>		T98371	15036	<i>KIAA0160</i>		D63881	170329
<i>CPD</i>	carboxypeptidase D	U65090	5057	<i>SH3GLPI-M</i>	SH3-domain GRB2-like 1 pseudogene	X99658	
<i>SHGC-33050</i>		G29398		<i>WI-9461-M</i>		G07297	183294
<i>GOS28</i>	golgi SNAP receptor complex member 1	AF073926	8868	<i>sSG31654-M</i>		AA910341	191479
<i>SH3GLP2-P</i>	SH3-domain GRB2-like 1 pseudogene	X99660		<i>sSG-40093-M</i>		AI378068	124418
<i>WI-9461-P</i>		G07297	183294	<i>WI-12393-M</i>	mod. similar to KIAA0563 protein	G20446	14232
<i>sSG31654-P</i>		AA910341	191479	<i>SHGC-17169</i>		G19390	192761
<i>sSG40093-P</i>		AB780808	124418	<i>KIAA0727</i>	similar to unconventional myosins	AB018270	39871
<i>WI-12393-P</i>	mod. similar to KIAA0563 protein	G20446	14232	<i>CDK5R1</i>	CDK5 regulatory subunit 1/p35	X80343	2869
<i>CYTOR4</i>	cytokine related receptor protein 4	G30528	119410	<i>WI-16331</i>		G20991	120762
<i>sts-N67026</i>	weakly similar to AD7C-NTP	N67026	206654	<i>sSG42502</i>		H86705	40488
<i>SHGC-33441</i>		T70563		<i>sSG28748</i>		AA860832	
<i>sSG12855</i>		H56424	221463	<i>sSG48313</i>		AA279265	97128
<i>N22706</i>		N22706	43234	<i>sSG13199</i>		H75373	
<i>SHGC-35907</i>		D19648	94891	<i>sSG39802</i>		AA084612	125286
<i>SHGC-34232</i>	weakly similar to IP4/PIP3 binding prot.	G28215	28802	<i>sSG60067</i>		AI017068	131740
<i>SHGC-35088</i>		H79008		<i>ZNF207-like</i>	zinc finger transcription factor	AF046001	62112
<i>FB12A2</i>		T02847		<i>SGC33551</i>	H. sapiens clone 23685 mRNA seq.	AF052093	9800
<i>NF1</i>	neurofibromin	M89914	93207	<i>p44.5/PMSD11</i>	macropain 26S proteasome subunit	AB003102	90744
<i>OMG</i>	oligodendrocyte myelin glycoprotein	M63623	194772	<i>R22783</i>		R22783	
<i>EV12A</i>	ecotropic viral integration site	M55267	41846	<i>SHGC-2662</i>	weak sim. to ubiquitin-like protein 8	D11824	109701
<i>EV12B</i>	ecotropic viral integration site	M60830	5509	<i>sis-H81937</i>	mod. sim. to serine/threonine kinase	H81937	37528
<i>AK3-p1</i>	adenylate kinase pseudogene	X60674		<i>SHGC-32151</i>	weak similarity to RAS gene family	AA199845	14202
<i>N25049</i>	expressed only in olfactory epithelium	N25049	183219	<i>ACCN1</i>	sodium channel (hBNAc1), degenerin	U57352	6517
<i>sts-M79255</i>		M79255		<i>TADA1</i>	maid-like gene	N37022	3447
<i>IB518</i>	weakly similar to KIAA0665 protein	T03582	3454	<i>sSG50857</i>		AA400117	125747

Genes and ESTs in bold are within the 1.5 Mb commonly deleted NF1 region

Table 4. Physical features of subjects with *NF1* microdeletions

Patient ID ¹	Cutaneous neurofibromas ²		Ht ³	Macrocephaly (cm)	Facial Features	Intelligence ⁴	Hands / Feet	Heart ⁵	Other Tumors	
	Age	Number							Type, Number	Age
Patients with deletion breakpoints at NF1REP-P and NF1REP-M										
69-3	8	many	5%	-(54.5)	hypertelorism	IQ 59	"normal"		plexiform neurofibroma, 2	10
119-1	22	TNTC	50%	+	hypertelorism	IQ 80s "dull normal"	NI	-		
123-3	5	many	Nml	+	hypertelorism, Ptosis	LD	25-50%	ASD	plexiform neurofibroma, 1 neurofibrosarcoma, 1	5 9
128-3	7 29	Several TNTC	3%	-(55)	Ptosis, downslanting palpebral fissures	normal		10-25%		
147-3	6	numerous	40%	-	Hypertelorism, ptosis, coarse, downslanting palpebral fissures	significant delays	NI	-		
156-1	31	TNTC	NI	NI	"dysmorphic"	mild MR with severe LD	NI	-	optic glioma	
160-1	11 35	Several TNTC	<3%	NI	"Noonan-like," coarse	LD, special education	NI	-	plexiform neurofibroma, 1	7
166-1	39	TNTC	NI	NI	telecanthus, downslanting palpebral fissures	"dull"	"large"	-		
166-2	7 19	Several TNTC	90%	-(56.5)	hypertelorism, downslanting palpebral fissures	special education	>97%	-		
166-3	4	none	NI	-(49)	downslanting palpebral fissures, "unusual face"	"normal", speech impediment	97%	-		
166-4	5 6	none 9	90%	-(48.5)	downslanting palpebral fissures	"normal", speech problems	97%	-		
167-1	4 7	7 20	NI	NI	ptosis, broad neck	mild development delay	NI	ASD, PS		

169-1	18	present	NI	+	coarse, hypertelorism, downslanting palpebral fissures	"dull normal," LD	"large"	Dilated aortic valve replaced	see footnote ⁶
172-1	childhood 35	None TNTC	NI	NI	"dysmorphic"	severe LD	"large"	-	optic glioma, 1 plexiform neurofibroma, 2
176-1	13	NI	10%	-	webbed neck, "Noonan"	WISC-III, mild/borderline MR	97%	-	plexiform neurofibroma, 2
183-1	12	10	25-50%	NI	hypertelorism, ptosis, broad nose	borderline development delay	50%	PS	plexiform neurofibroma, 1
184-1	5	TNTC	NI	NI	telecanthus, coarse face	IQ 71 fullscale, 81 verbal, 66 performance	97%	-	

Patients with at least one unique *NF1* deletion breakpoint

106-3	18	TNTC	Nml	+	(61.5)	coarse	IQ 46	"large"	-	plexiform neurofibroma, 1 spinal neurofibromas, TNTC	3 25
113-1	8 15	TNTC TNTC	10%	+	(59)	coarse, hypertelorism	IQ 88 LD	>97%	-	-	
155-1	27	TNTC	NI	+	(59.5)	coarse, ptosis	moderate MR	>97% hands 75% feet	-	spinal neurofibroma, 1 neurofibrosarcoma, 1 ⁷ see footnote ⁷	sym 27 28

¹The UWA- prefix for patient identifiers is not shown. All patients are unrelated, with the exception of 4 members of family UWA166.

²Age in years; TNTC, too numerous to count.

³Height in percentile; Nml, normal; NI, no information available.

⁴LD, learning disabilities; MR, mental retardation.

⁵PS, pulmonic stenosis; ASD, atrial septal defect.

⁶Patient's mother and sister with NF1, presumably due to the same NF1 microdeletion, had retroperitoneal fibrosarcoma with metastases (~age 30) and cerebellar medulloblastoma (age 16), respectively.

⁷Spinal neurofibroma was symptomatic at age 27; patient inherited NF1 from his father who died of malignant CNS tumor in 5th decade.

Table 5: Contiguous gene rearrangements involving low copy repeats

Disorder	Location	Rearrangement Type	Size (kb)	REP Size (kb)	Transcripts in REP	Reference
NF1	17q11.2	Del	1500	15-100	<i>SH3GLP</i> , <i>WI-9461</i> , <i>stSG31654</i> , <i>stSG40093</i> , <i>WI-12393</i>	this paper
VCFS/DGS CES (Cat eye syndrome)	22q11	Del Dup	2000/150 0	200	<i>GGT</i> , <i>GGT-rel</i> , <i>BCRL</i> , <i>V7-rel</i> , <i>POM121-like</i>	45, 48
Williams syndrome	7q11.23	Del	2000	>30	<i>GTF2I</i> , <i>IB1445</i>	47
HNPP CMT1A	17p11.2	Del Dup	1500	24	<i>COX10</i>	43
Smith-Magenis	17p11.2	Del	5000	200	<i>TRE</i> , <i>KER</i> , <i>SRP</i> , <i>CLP</i>	44
PWS/Angelman	15q11-13	Del	4000	50-200	<i>SGC32610</i> , <i>SHGC15126</i> , <i>SHGC17218</i> , <i>A006B10</i> , <i>MN7</i> , <i>A008B26</i> , <i>HERC2</i>	46, 49
NPHP1 (Nephronophthisis type 1)	2q12-13	Del	250	100	<i>D2S1735</i> , <i>D2S2087</i>	53



DEPARTMENT OF THE ARMY
US ARMY MEDICAL RESEARCH AND MATERIEL COMMAND
504 SCOTT STREET
FORT DETRICK, MARYLAND 21702-5012

REPLY TO
ATTENTION OF:

MCMR-RMI-S (70-1y)

23 Aug 01

MEMORANDUM FOR Administrator, Defense Technical Information
Center (DTIC-OCA), 8725 John J. Kingman Road, Fort Belvoir,
VA 22060-6218


SUBJECT: Request Change in Distribution Statement

1. The U.S. Army Medical Research and Materiel Command has reexamined the need for the limitation assigned to the technical reports listed at enclosure. Request the limited distribution statement for these reports be changed to "Approved for public release; distribution unlimited." These reports should be released to the National Technical Information Service.

2. Point of contact for this request is Ms. Judy Pawlus at DSN 343-7322 or by e-mail at judy.pawlus@det.amedd.army.mil.

FOR THE COMMANDER:

Encl


PHYLLIS M. RINEHART
Deputy Chief of Staff for
Information Management

Reports to be Downgraded to Unlimited Distribution

ADB241560	ADB253628	ADB249654	ADB263448
ADB251657	ADB257757	ADB264967	ADB245021
ADB263525	ADB264736	ADB247697	ADB264544
ADB222448	ADB255427	ADB263453	ADB254454
ADB234468	ADB264757	ADB243646	
ADB249596	ADB232924	ADB263428	
ADB263270	ADB232927	ADB240500	
ADB231841	ADB245382	ADB253090	
ADB239007	ADB258158	ADB265236	
ADB263737	ADB264506	ADB264610	
ADB239263	ADB243027	ADB251613	
ADB251995	ADB233334	ADB237451	
ADB233106	ADB242926	ADB249671	
ADB262619	ADB262637	ADB262475	
ADB233111	ADB251649	ADB264579	
ADB240497	ADB264549	ADB244768	
ADB257618	ADB248354	ADB258553	
ADB240496	ADB258768	ADB244278	
ADB233747	ADB247842	ADB257305	
ADB240160	ADB264611	ADB245442	
ADB258646	ADB244931	ADB256780	
ADB264626	ADB263444	ADB264797	